Chapter 3. C-C Oxidative Cross-Coupling of Phenols

Contents

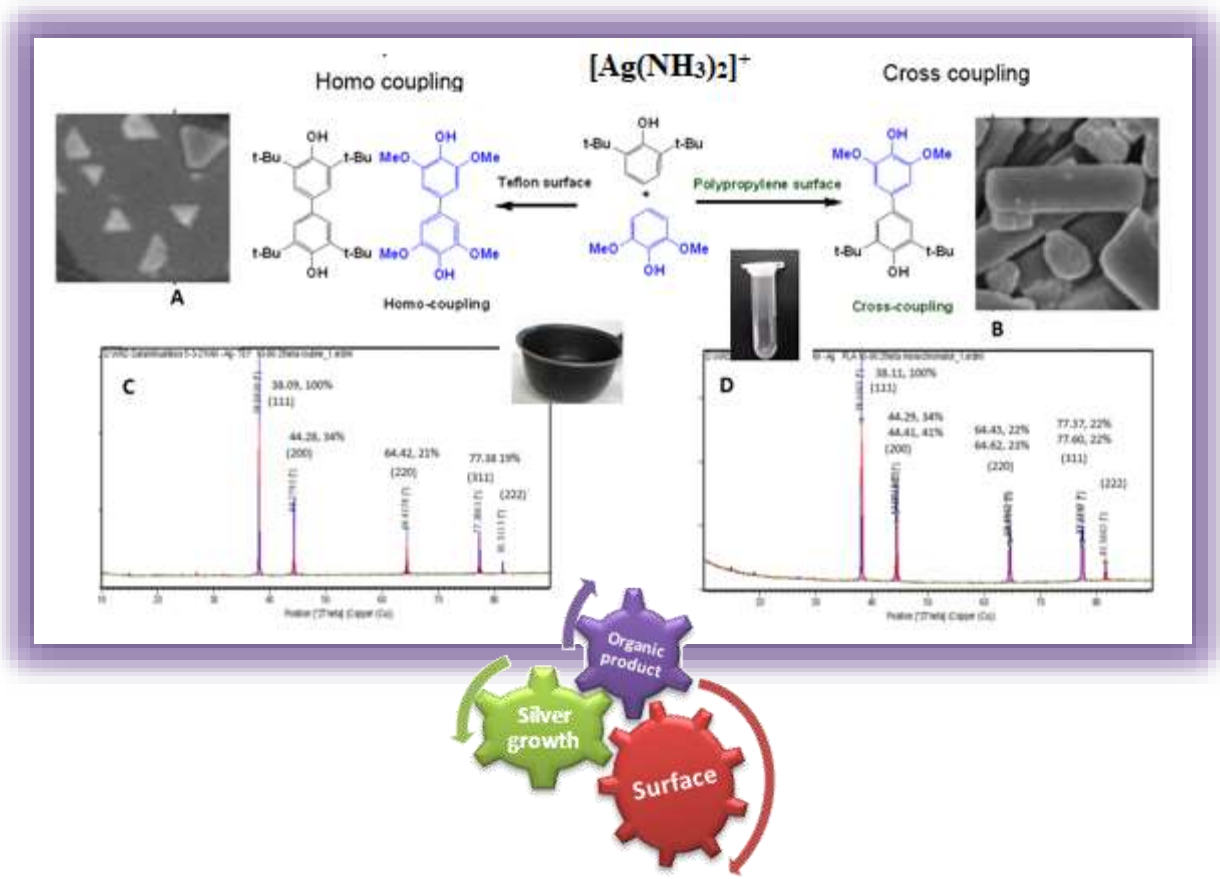

Abstract

This chapter describes the **C-C oxidative cross-coupling** of phenol and naphthol derivatives by slightly modifying Tollens' reaction. Total six-coupled products were obtained quantitatively out of 28 cross-coupling reactions using Tollens' reagent. Then a study was converged on a curious experiment, where coupling reaction carried out in plastic or (polypropylene) surface resulted in the suspended silver particle formation over the typical formation of a silver mirrored film. This result prompted us to carry out the reaction, on different surfaces, such as borosilicate glass, Teflon, Eppendorf tube, etc., and 'observe' possible selectivity in the organic product formation. Surprisingly, the cross-coupling selectivity was observed by ONLY changing the surface of the reaction medium. The reaction between 2,6-dimethoxyphenol and 2,6-di-*tert*-butylphenol yielded a cross-coupled product 10% in plastic and 70% in teflon. This prompted us to study, the silver particles formed during these reactions using optical microscopy, FE-SEM, and P-XRD analysis. Thus, the study highlights, and discusses, the importance of the growth of metallic silver aggregation and its role during concurrent chemo-selective oxidative coupling product formation.

3.1 Introduction

The **cross-coupling** processes were investigated from the beginning of the 19th century; still, research in this field is challenging. One of the best examples, palladium-catalyzed cross-coupling reactions developed by Richard Heck, Eiichi Negishi, and Akira Suzuki, Nobel Prize in 2010.[1] Thus, the role of transition metal-catalyzed cross-coupling reactions have been reported to prepare biaryl bonds (Ar-Ar') with precise selectivity and high chemical yield.[2] Herein, to establish the chemo-selectivity, two activated arene units should be substituted before coupling mainly with inverted electronic nature (Ar-X and Ar'-M) as shown in the general scheme S3.1.1. Consequently, the entire synthesis becomes lavish due to the involvement of multiple sequences of reaction such as protection and deportation, which makes it inefficient in terms of the atom- and step-economy results in large quantitative toxic waste.

Scheme S3.1.1: General scheme for Transition metal-catalyzed cross-coupling reaction

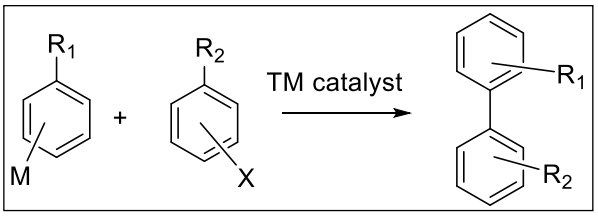

Alternatively, **oxidative coupling** reactions offer **a single-step approach** for preparing biaryl bonds by merging two unfunctionalized arenes.[1] Here preferred homo-coupling by-product formation under the normal reaction conditions makes cross-coupling quite challenging. In literature, different strategies have been reported to improve reaction selectivity, as shown in scheme S3.1.2.

(1) Choosing appropriate phenols: **Kočovský** et al. proposed a sufficient difference in redox potentials (i.e., if $\Delta E_{ox} > 0.25$ V) in the phenolic coupling partners favors cross-coupling.[3,4] In the previous report **Hovorka and Zavada** also realized a similar trend. But, the role of catalyst and solvent remained elusive during the reaction mechanism.[5,6]

(2) Use of metal complexes: **Kozlowski's** et al. studied the catalytic activity of several M[sale(a)n] complexes (M = Fe, V, Cr, and Mn) under aerobic conditions and identified Cr[salen] as a suitable catalyst for the oxidative cross-coupling of phenols, which increases intra-molecular coupling through a cooperative (particles) model.[3,4,7]

(3) Use of sterically hindered phenols: **Waldvogel** et al. explored the electrochemical process for cross-coupling of phenols, where the selectivity was obtained by choosing sterically

hindered groups on phenols.[8,9] Metal-free cross-coupling has been reported with hypervalent iodine reagents and sulphoxide catalyzed reactions.[10,11] The requirement of phenols in different stoichiometric other than 1:1 and fluorinated solvents have been reported, but the reasons were not given.[8,9,12,13]

Scheme S3.1.2: Selected examples of oxidative cross-coupling reaction reported by different research groups to achieve cross-coupling chemo-selectivity

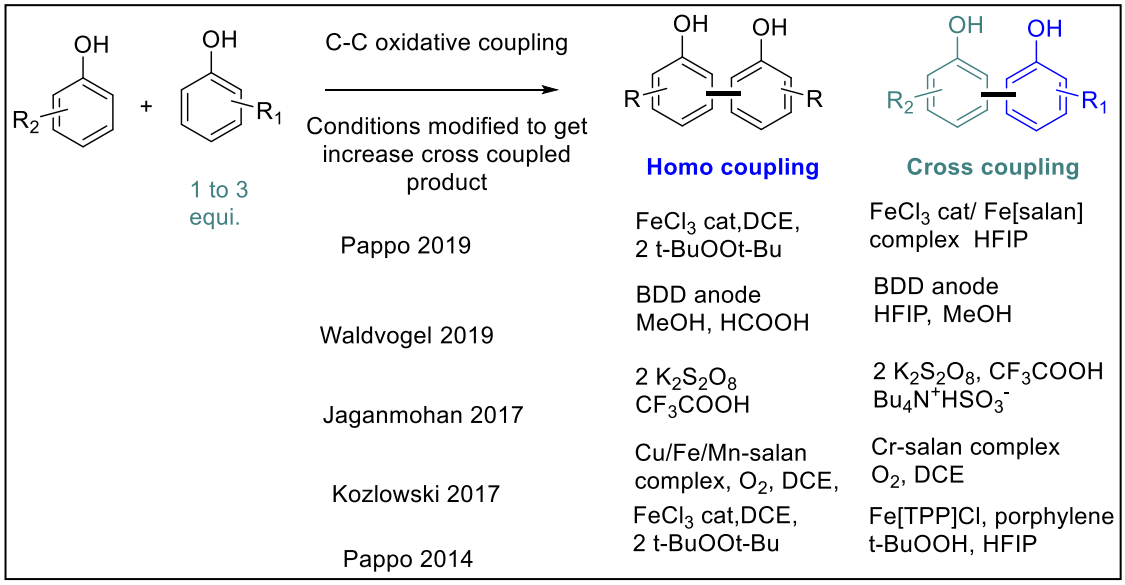

(4) Use of fluorinated solvent: **Pappo** et al. systematically studied several cross-coupling reactions of phenols using iron (and copper) salen and porphyrin complex and reported chemo-selectivity in the presence of a fluorinated solvent.[6,14–16] Pappo group proposed, fluorinated solvent forms strong hydrogen-bonded assemblies amongst the most redox-active phenol derivative and then nucleophilic attack by the other phenol in the micro-heterogeneous environment. [14–17] Later on, **Jaganmohan** reported the selectivity of certain phenols toward the cross-coupling by using a fluorinated solvent.[18]

This hypothesis was debated by **Kocovsky** et al., especially with iron chloride and peroxide reagent for obtaining cross-coupling product between 2,6-dimethoxyphenol and 6-Bromo-2-naphthol in HFIP and MDC solvents. They observed particular combinations were only giving cross-coupling results.[3,16]

The Pappo group proposed a mechanistic pathway, as shown in Figure F3.1.1. They proposed cross-coupling of two phenols containing different oxidation potentials $\mathbf{E_{ox}(A) < E_{ox}(B)}$ has three possibilities for coupling. Single-electron transfer reaction prefers free radical-radical

coupling reaction mechanism and results in thermodynamically preferred homo-coupling product formation.[16] The radical-anion coupling mechanism could result in homo and cross-coupled product formation if the nucleophilicity of phenol having higher oxidation potential contains less nucleophilic character than other ($N_B > N_A$) and vice versa ($N_A > N_B$), respectively.[5,6,13,16] They proposed nucleophilic character of phenol can be varied by using a fluorinated solvent system to obtain chemo-selectivity.[16] The nucleophilic character at the *ortho*-position of methoxy group increases due to strong intermolecular hydrogen bond between HFIP and phenolic hydroxide than intra-molecular hydrogen bonding. However, the basic principles guiding cross-coupling selectivity in these oxidation systems remained unclear.[15,16,19]

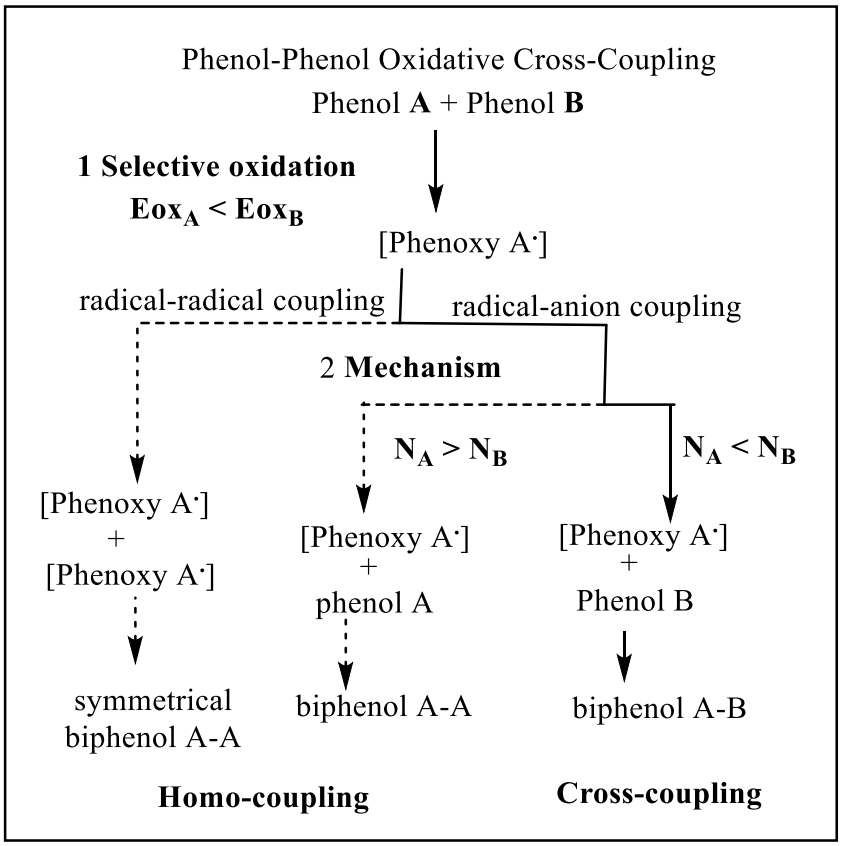

Figure F3.1.1: Model for predicting cross-coupling selectivity in oxidative cross-coupling of phenols: 1. selective oxidation of phenol-A; 2. Radical-anion coupling mechanism and selectivity based on nucleophilicity of phenol-B.

All these strategies control molecular interactions, predominantly favoring radical-anion interaction over radical-radical and radical-cation interactions.[9,12,19–21] With this background, the role of Tollens' reagent in chemo-selectivity in a cross-coupling reaction has been undertaken.

Tollens' on different work, **surface-assisted reactions** have attracted researchers and are considered an emerging area of research. It has been considered curious and practical due to its great potential for the novel synthesis of complex structures with well-defined architectures with specific purity.[22] Nowadays, catalytically active surfaces are getting generated for selectivity, efficiency, easy dissociation ability of the reactant, and less binding ability of intermediates.[23] Specific product formation has been reported by changing surface even though multiple chemical active sites in the reagent, as shown in scheme S3.1.3; for example, 7,7-dibromo-2,2-binaphthol reaction on the silver surface and gold surface resulted in cyclized and polymeric molecule formation respectively, due to the intermolecular and intra-molecular bond formation.[24] Apart from that, the shape or facet of catalyst also acts as active sites, which has been considered selectivity factors; For example, benzene reduction on platinum catalyst surface resulted in selectively cyclohexane formation over (111) and the

Scheme S3.1.3: Selected examples from literature showing role of surface on reaction selectivity

A. different metal surface B. Role of active face C. Role of metal particle size

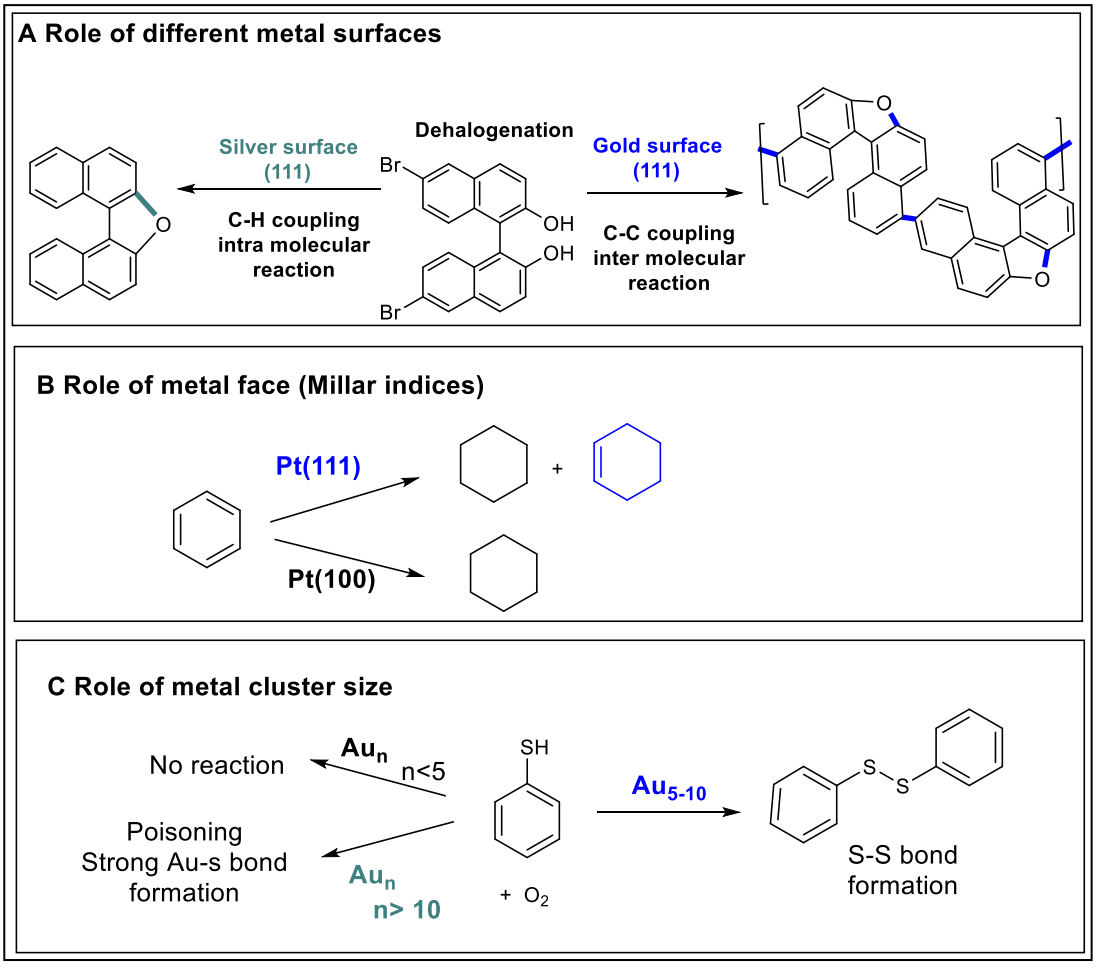

mixture of cyclohexane and cyclohexene over (100) facet.[25] Interestingly the shape of particles or clusters varies depending on crystalline facets, and thus different reactivity and chemo-selectivity were observed in organic transformation. Water-gas formation reaction reported with rod shape silver nanoparticle resulted with less selectivity than cubic shape; due to requirement of high activation energy on (111) facets than (100).[26] The size of particles also leads to product selectivity. Three different clusters of gold particles, below five atoms, 5-10 atoms, and more than 10 atoms resulted in no reaction, desired S-S coupling, and poisoning of Au (due to Au-S strong bond formation), respectively.[27,28] Similarly, oxidation of styrene is reported, where the size of the silver cluster (25 to 144) is used as a catalyst for achieving chemo-selectivity of the oxidized product which varies from benzaldehyde, styrene epoxide, to acetophenone.[28–30]

How surface is generated?

Scheme S3.1.4: lateral versus vertical growth of silver nanoparticle by changing capping agent

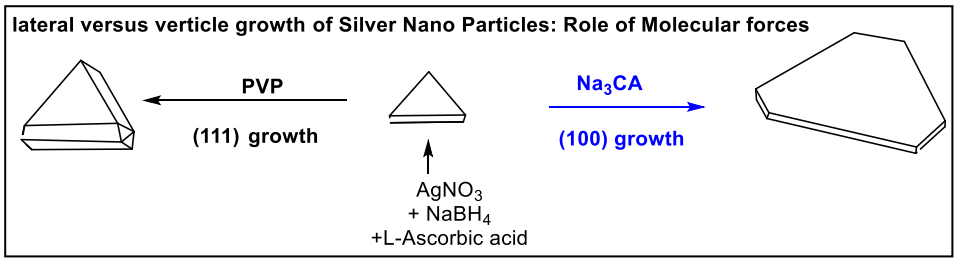

The metal clusters of desired geometry and size are commonly obtained by controlling the growth/ attachment of atoms. The generation of these surfaces has been reported in two ways: breaking giant clusters or joining small particles/ atoms, known as bottom-up and top-down strategies.[31–33] The top-down approach is not as popular (although used by industries), because of the unknown bulk properties of clusters and the difficulty in uniform splitting. On the contrary, the bottom-up approach has been widely used and studied for nanoparticle synthesis by adding capping agents in redox reaction mixtures.[33,34] The variation in the shape and size of the reduced products has been reported by changing the capping agents, as shown in scheme S3.1.4.[33,35,36] Apart from this, many fundamental factors such as the interplay of the solution, reaction dynamic, and kinetic processes that interfere with nucleation and growth of particles. The cohesive forces also affect the adhesion of solid, which varies along with its type, the elasticity of solid, roughness, surface angle, and wetting ability size, thus ultimately surface energy.[37,38]

Traditionally, the focus in oxidative C-C oxidative coupling reaction remains on the stability of the intermediate or the oxidized organic product formation while the role or fate of the reduced component remained unexplored. This prompted the present study to focus on the growth of silver formation and its correlation to the C-C oxidative coupling.

3.2 Present strategy

i. Efforts were directed on using Tollens' reagent for exploring chemo-selectivity in C-C oxidative cross-coupling reactions of phenol and naphthol derivatives.

ii. To achieve chemo-selectivity, reactions were studied using a fluorinated solvent.

iii. Optimization of cross-coupling reaction condition and proposed mechanism.

iv. Curious Experiment- Changing the surface of reaction Vessel from borosilicate glass to plastic/teflon and correlating its effect on selective C-C oxidative cross-coupling reaction.

3.3 Result and Discussion

Scheme S3.3.1: General scheme for cross coupling reaction of phenol derivatives using Tollens' reagent

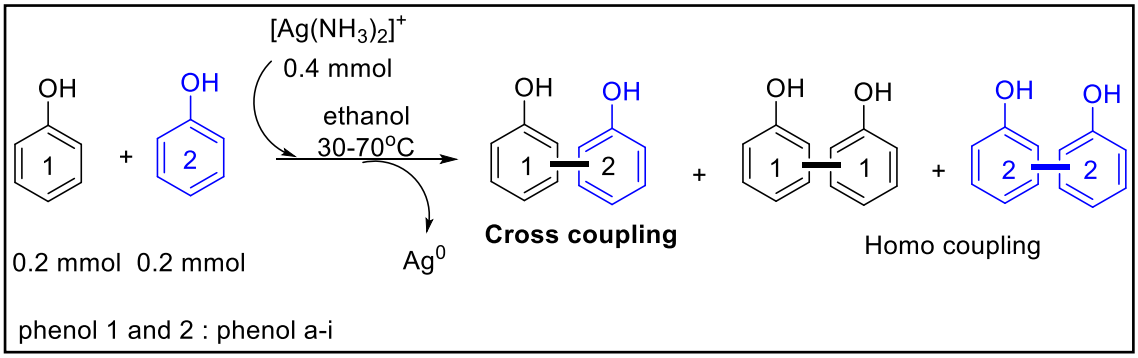

The cross-coupling reaction of phenol and naphthol derivatives was attempted using Tollens' reagent, as shown in scheme S3.3.1 (Refer to section 3.5.3 for detailed experimental procedure). Total nine Phenol and naphthol derivatives were used to study cross-coupling reactions, which includes 2-naphthol (**a**), 2,7-dihydroxynaphthalene (**g**), 2,4-di-*tert*-butylphenol (**b**), 2,6-di-*tert*-butylphenol (**c**), 2,4-di-methylphenol (**d**), 2,6-di-methylphenol (**h**), 2,6-di-methoxyphenol (**e**) and 2-*tert*-butyl-4-methoxyphenol (**f**). Unfortunately, Phenol-**f**, 4-methylphenol (**g**), 4-*tert*-butylphenol (**h**), and 6-Bromo-2-naphthol (**i**) in cross-coupling reaction resulted in the multiple unknown by-products thus not investigated further. C-C

	Name								
1	2,6-dimethoxy phenol	HC							
2	2-tertbutyl-4methoxy phenol	X	HC						
3	2,4-dimethyl phenol	X	-	HC					
4	2-naphthol	√	-	X	HC				
5	2,6-dimethyl phenol	√	-	X	X	HC			
6	2,6-ditert butyl phenol	√	X	√	√	√	HC		
7	2,4-ditert butyl phenol	X	-	X	X	X	X	HC	
8	2,7-dihydroxy naphthalene	X	-	X	√	-	X	X	HC
	Name	2,6-dimethoxy phenol	2-tertbutyl-4-methoxy phenol	2,4-dimethyl phenol	2-naphthol	2,6-dimethyl phenol	2,6-ditert butyl phenol	2,4-ditert butyl phenol	2,7-dihydroxy naphthalene

√ = CROSS-COUPLING PRODUCT
X = ONLY HOMO-COUPLING PRODUCT
- = MULTIPLE PRODUCTS
HC = HOMO-COUPLING REACTION

Figure F3.3.1: Coupling reaction of phenol derivatives in tabulated form

oxidative coupling is observed mainly in vacant *ortho* and *para* positions depending on the vacant site available for coupling, as shown in table T3.1. The phenol derivatives needed 30 minutes for complete conversion, but naphthol derivatives needed 2-3 days at 30°C, which may be due to dissimilarity in reactivity. Thus, the cross-coupling reactions of naphthol derivatives with phenol derivatives were preferentially carried out at 70°C. In some cases, minor cross-coupled products were observed, mainly on TLC, and analyzed using mass spectrometry. However, only six cross-coupled products could be obtained quantitatively out of 28 combinations, using the general procedure of cross-coupling by silver ammine complex, as noted in Figure F3.3.1. The products were characterized by FT-NMR (^{1}H and ^{13}C) spectroscopy (Figures F3.6.1 to F3.6.6), FT-IR spectroscopy (Figures F3.6.14 to F3.19), and Mass spectrometry analysis (Figures F3.6.7 to F3.13), as shown in section 3.5.17.

Table T3.1: C-C oxidative cross-coupling reaction carried out with phenols*

Phenol-1 [I]	**Phenol-2** [II]	**Tem** [III]	**Time** [IV]	**Cross-coupled Products if formed otherwise observed homo-coupled product** [V]	**The yield of cross-coupled product** [VI]
a	b	70°C	3hr	1-(3,5-di-*tert*-butyl-2-hydroxyphenyl)-2-naphthol **(1ab)**	Minor
	c	70°C	3 hr	1-(4'-Hydroxy-3',5'-di-*tert*-butyl phenyl)-2-naphthol **(1ac)**	10%
	d	70°C	3hr	1-(2-hydroxy-3,5-dimethylphenyl)-2-naphthol **(1ad)**	Minor
	e	70°C	3 hr	1-(4'-Hydroxy-3',5'-dimethoxyphenyl)-2-naphthol **(1ae)**	8%
	g	30°C	3 day	1,1'-binaphthyl-2,7,2'-triol **(1ag)**	12 %
		70°C	3hr		16%
	h	70°C	3 hr	3,5-di-*tert*-butyl-3',5'-di-methyl-(1,1'-biphenyl)-4,2'-diol **(1ah)**	Minor
b	c	30°C	60 min	Only Homo-coupling	-
	d	30°C	60 min	Only Homo-coupling	-
	e	30°C	60 min	3,5-di-*tert*-butyl-3',5'-dimethoxy-2',3'-dihydro-(1,1'-biphenyl)-2,4'-diol **(1be)**	Minor
	g	70°C	3hr	Only Homo-coupling	-
	h	30°C	30 min	Only Homo-coupling	-
c	d	30°C	60 min	3,5-di-*tert*-butyl-3',5'-di-methyl-(1,1'-biphenyl)-4,2'-diol **(1cd)**	9%
	e	30°C	60 min	3,5-di-*tert*-butyl-3',5'-di-methoxy-(1,1'-biphenyl)-4,4'-diol **(1ce)**	58%
	f	30°C	60 min	Homo-coupling with multiple spots	-
	g	70°C	3hr	Only Homo-coupling	-
	h	30°C	60 min	3,5-di-*tert*-butyl-3',5'-di-methyl-(1,1'-biphenyl)-4,4'-diol **(1ch)**	Minor
d	e	30°C	60 min	Only Homo-coupling	-
	f	30°C	60 min	Homo-coupling with multiple spots	-
	g	70°C	3hr	Only Homo-coupling	-
	h	30°C	30 min	Only Homo-coupling	-
e	f	30°C	60 min	Homo-coupling with multiple spots	-
	g	70°C	3hr	Homo-coupling with multiple spots	-
	h	30°C	30 min	3,5-di-methoxy-3',5'-di-methyl-(1,1'-biphenyl)-4,4'-diol **(1eh)**	16%

*Where reaction of [(I) and (II)] phenol derivatives 0.2 mmol of each were carried out using reaction conditions (III-IV): [(III)] Temperature of reaction, [(IV)] time for reaction; [(V)] cross-coupling product if formed; [(VI)] isolated column purified cross-coupled yield

Choosing correct combinations of phenols for cross-coupling reaction

Phenols and naphthol derivatives were arranged in the global nucleophilicity N_o versus oxidation potential E_{ox} graph[6], as shown in Figure F3.3.2. (These values of N_o were reported in the Pappo group by the DFT method, and E_{ox} was experimentally determined using the CV method.[6]) Any strong correlation of N_o and E_{ox} on coupling selectivity was not observed in the C-C oxidative coupling reaction using Tollens' reagent F3.3.2, and due to the more preferred homo-coupling by-product formation under the given reaction conditions. Phenol-e, phenol-h, and phenol-c have E_{ox} 0.40 V, 0.54 V, 0.92 V, and N_o 3.75 eV, 3.35 eV, and 3.4.3 eV respectively; thus, they were selected to investigate the mechanism of cross-coupling reaction of phenol with modified Tollens' reagent.

Figure F3.3.2: Relativity map of phenols based on E_{ox} and N_o values* (phenol, E_{ox}, N_o);

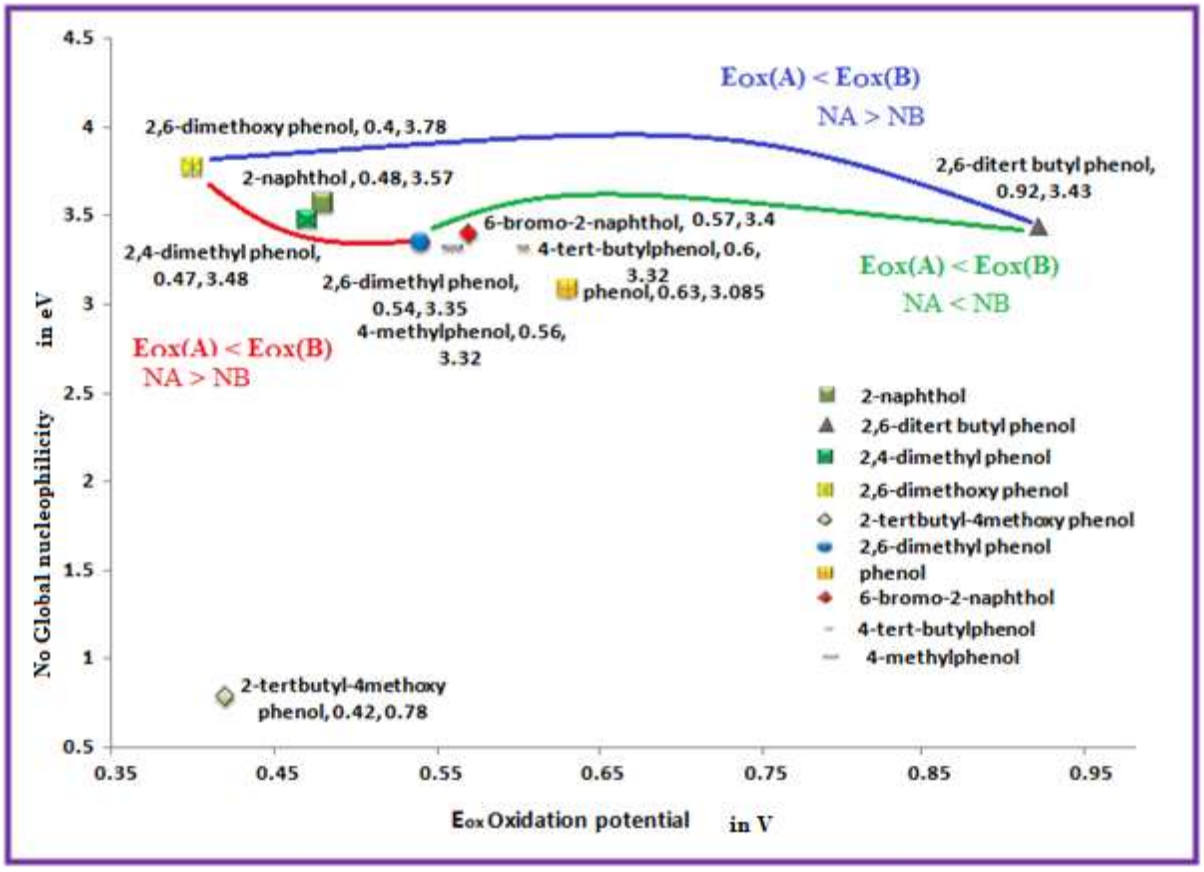

* three combinations/pairs of phenols were chosen for the mechanism study are connected with lines: Herein E_{ox} 2,6-dimethoxyphenol < E_{ox} 2,6-dimethylphenol < E_{ox} 2,6-di-tert-butylphenol, and N_o 2,6-dimethoxyphenol > N_o 2,6-di-tert-butylphenol > N_o 2,6-dimethylphenol (In the image A is considered as a phenol having higher oxidation potential than B).

Effect of the stoichiometric amount of phenols in C-C oxidative cross-coupling reaction

Scheme S3.3.2: Effect of the stoichiometric amount of phenols on chemo-selectivity in the cross-coupling reaction of phenol c with e

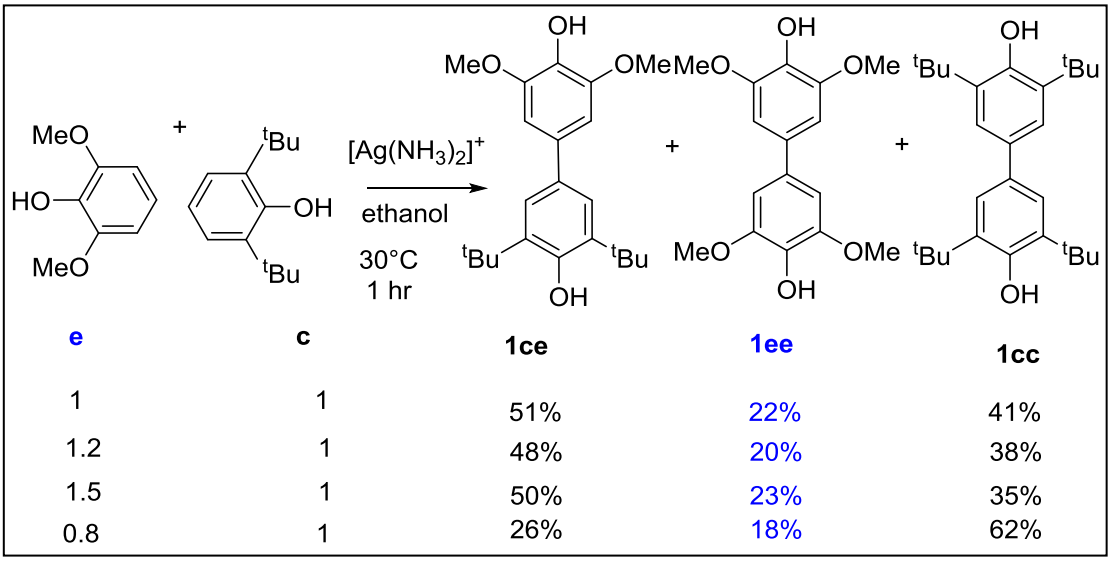

e	c	1ce	1ee	1cc
1	1	51%	22%	41%
1.2	1	48%	20%	38%
1.5	1	50%	23%	35%
0.8	1	26%	18%	62%

According to literature, cross-coupling product formation can be favored over homo-coupling by adding the least oxidizable phenol in significantly excess than a phenolic partner (phenols with oxidation potential difference more than 0.25 eV).[6,16] Accordingly, the coupling of phenol-c with phenol-e ($N_{o\ phenol\text{-}e} < N_{o\ phenol\text{-}c}$) was carried out by varying the stoichiometry amount of phenol-e (1.0/ 1.2/ 1.5/ 0.8 mole Equiv.) shown in scheme S3.3.2 (Refer section 3.5.3.1 for detailed experimental procedure). The yield of 1ce remained consistent even by increasing the amount of less nucleophilic phenol-e. But overall, products decrease with decreasing phenol-e in reaction. The poor chemo-selectivity in cross-coupling products due to competitive homo-coupling products was observed herein and showed 1:1 phenol partners are preferred for the coupling reaction.

Effect of reaction temperature

Scheme S3.3.3: Effect of temperature on chemo-selectivity in the cross-coupling reaction of phenol-c with e

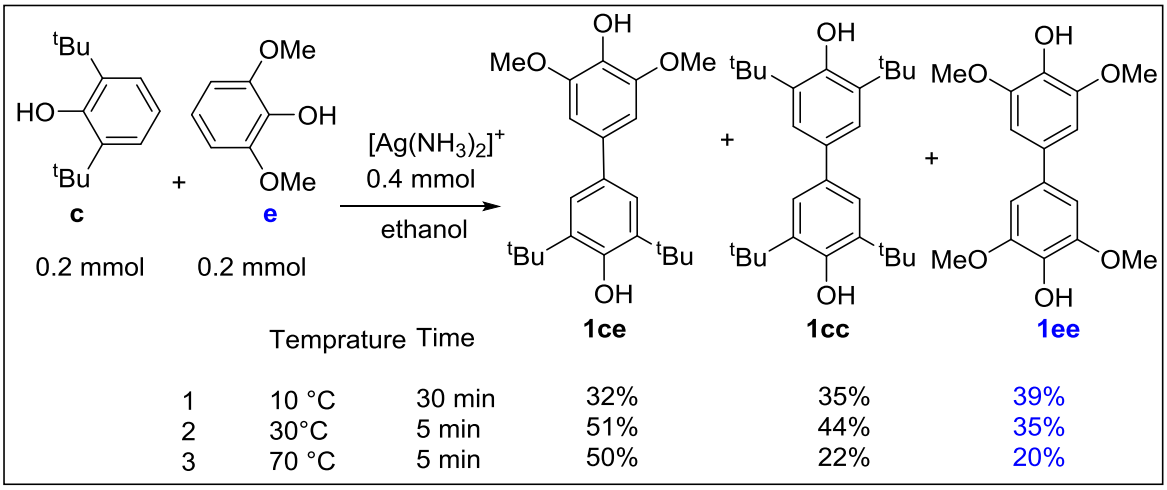

Cross-coupling reactions of phenol-c with e were performed at different reaction temperatures 10°C, 30°C, and 70°C, as shown in scheme S3.3.3 (Refer to section 3.5.3.2 for detailed experimental procedure). On cooling the reaction from 30°C to 10°C, the yield of 1ce was decreased from 51% to 32%. Herein the selectively homo-coupling products were formed, and the starting material has also remained un-reacted. On the other side, homo-coupling product decreased, and 1ce yield remained intact on the increasing temperature of the reaction from 30°C to 70°C, as shown in Figure F3.3.3-1. The time required for complete consumption of silver nitrate was about 30 minutes, 5-7 minutes, and 5 minutes at a temperature of 10°C, 30°C, and 70°C, respectively. The results show kinetically and thermodynamically controlled chemo-selectivity.[6,16]

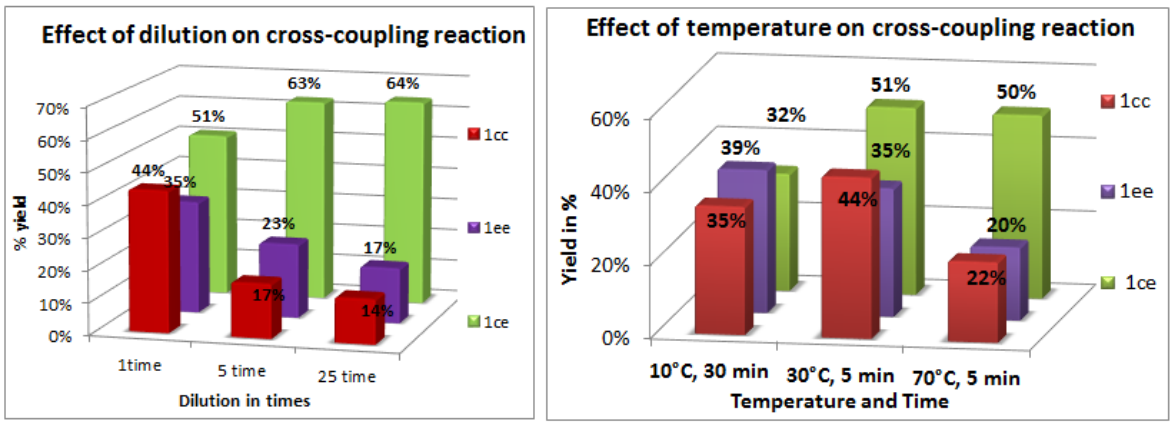

Figure F3.3.3: Coupling product (1ce, 1cc, and 1ee) yields versus change in condition 1. dilution of the reaction mixture (right) and 2. temperature of reaction (left)

Effect of change in concentration of the reaction

Dilute reaction conditions are considered as a critical factor in observing chemo-selectivity especially for radical intermediate forming reactions. Therefore, cross-coupling reactions of phenol-c with e were carried out in different dilutions as shown in scheme S3.3.4 (Refer to section 3.5.3.3 for detailed experimental procedure). On dilution of the reaction mixture from 0.4 ml to 2.0 ml, the yield of 1ce increased from 51% to 63%, whereas the yield of homo-coupling product 1cc significantly decreased from 44% to 17%. 64% 1ce was obtained on further 25 times dilution. In contrast, a minor increase in the homo-coupling was observed, as shown in Figure F3.3.3-2 in the graphical presentation. Thus, the selectivity in cross-coupling increased on dilution, but with some limit, also affects (increasing) time for conversion.

Scheme S3.3.4: Effect of dilution on chemo-selectivity in the cross-coupling reaction of phenol-c with e

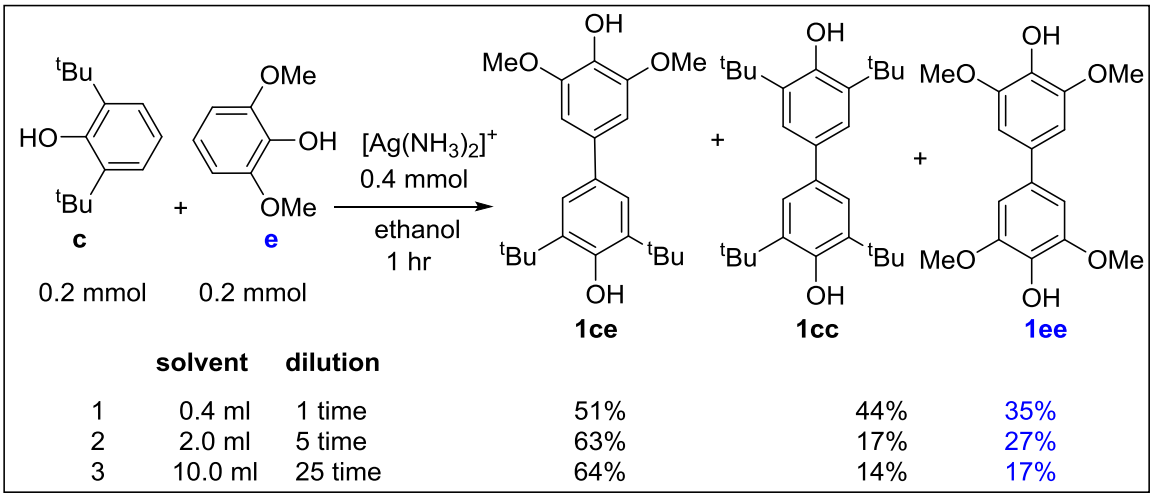

	solvent	dilution	1ce	1cc	1ee
1	0.4 ml	1 time	51%	44%	35%
2	2.0 ml	5 time	63%	17%	27%
3	10.0 ml	25 time	64%	14%	17%

Effect of addition of HFIP solvent in the cross-coupling reactions

Scheme S3.3.5: Effect of HFIP solvent on chemo-selectivity in the oxidative cross-coupling reaction of phenol-c with e

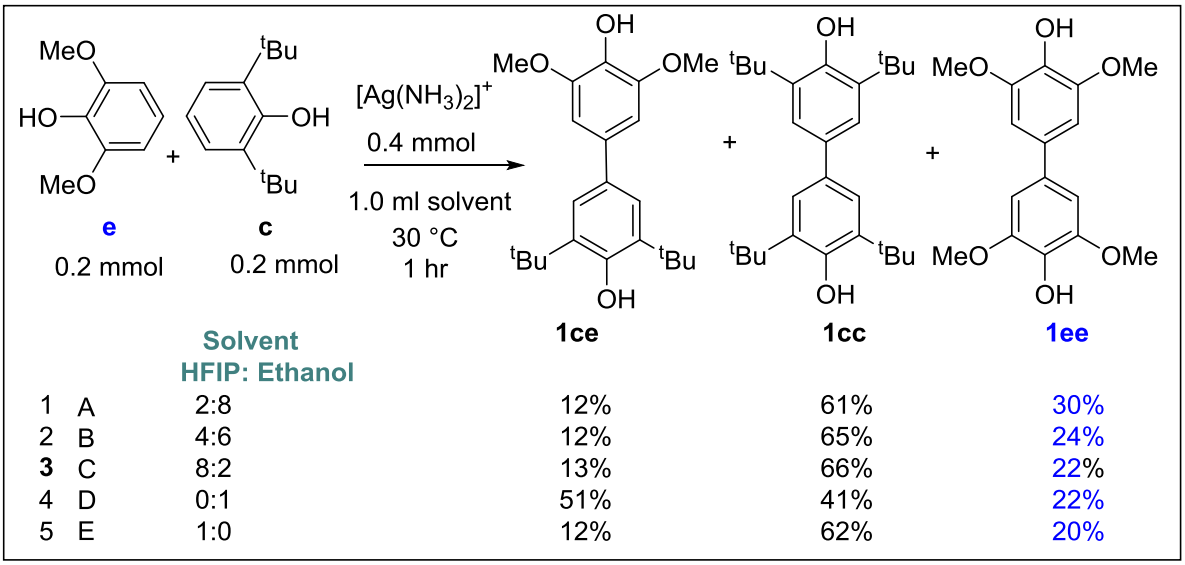

		Solvent HFIP: Ethanol	1ce	1cc	1ee
1	A	2:8	12%	61%	30%
2	B	4:6	12%	65%	24%
3	C	8:2	13%	66%	22%
4	D	0:1	51%	41%	22%
5	E	1:0	12%	62%	20%

According to Kocovsky and Pappo's group's experimental facts, adding a fluorinated solvent in cross-coupling of phenol-c and e results in cross-coupling product formation with a radical-anion coupling mechanism, where $E_{ox\ phenol\text{-}e} < E_{ox\ phenol\text{-}c}$ and $N_{o\ phenol\text{-}e} > N_{o\ phenol\text{-}c}$.[16] Cross-coupling of phenol-c and e with silver ammine complex was carried out in the presence of HFIP solvent, as shown in scheme S3.3.5 (Refer to section 3.5.4 for detailed experimental procedure). A slower conversion rate of silver ammine complex to silver was observed using HFIP solvent. A decrease in the yield of cross-coupling products by 40% was observed compared to the reaction carried out in ethanol solvent. Selective formation of 1cc (homo-coupling product) was observed. The *unreacted* phenol-e was also noted opposite to expected, as shown in Figure F3.3.4.

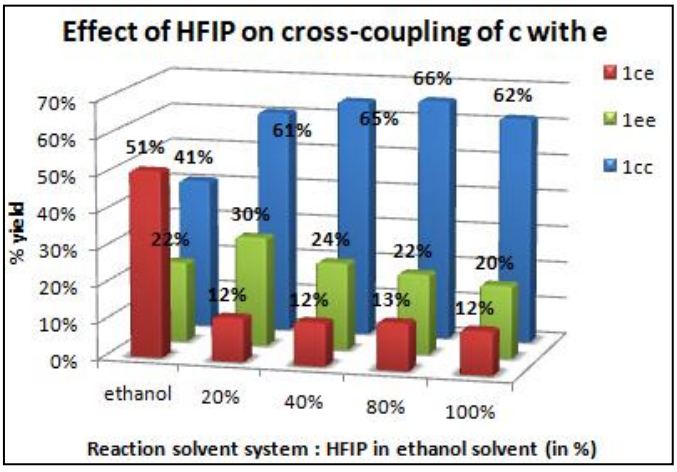

Figure F3.3.4 % yield of 1cc, 1ee, and 1ce products verses solvent (ethanol-HFIP) used for reaction

Scheme S3.3.6: Effect of HFIP in the C-C oxidative cross-coupling reaction of phenol e with h

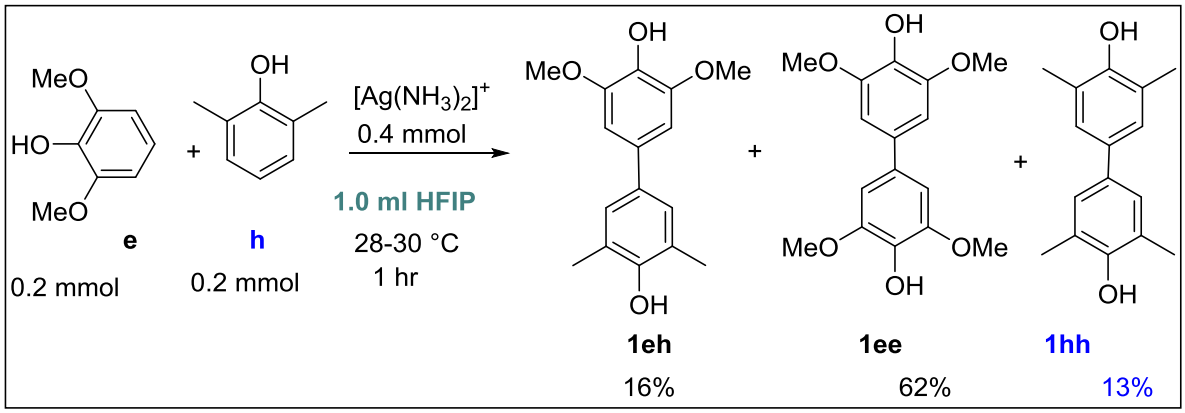

The Tollens' reaction of phenol-e with h was carried out with the addition of HFIP solvent, where the $E_{ox\ phenol\text{-}e} < E_{ox\ phenol\text{-}h}$ and $N_{o\ phenol\text{-}e} > N_{o\ phenol\text{-}h}$.[16] This reaction resulted in 16% 1eh formation, similar to ethanol solvent, as shown in scheme S3.3.6.

Scheme S3.3.7: Effect of HFIP in the cross-coupling reaction of phenol c with h

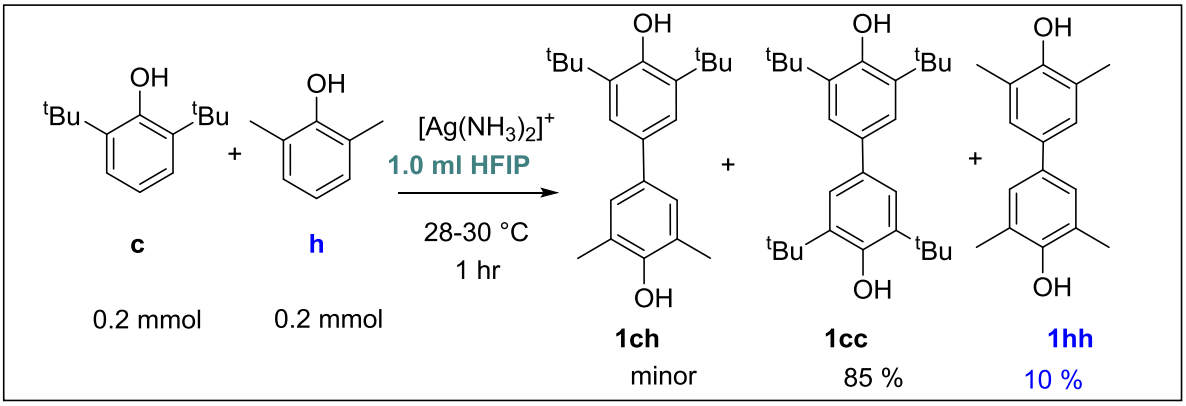

The cross-coupling of phenol-c with h in HFIP solvent was carried out using silver ammine complex, as shown in scheme S3.3.7. But, the yield of the cross and homo-coupling products were consistent even after adding HFIP solvent in this cross-coupling reaction of phenol-c with h.

Scheme S3.3.8: C-C oxidative coupling of phenol-e as a probe for determination of mechanism*

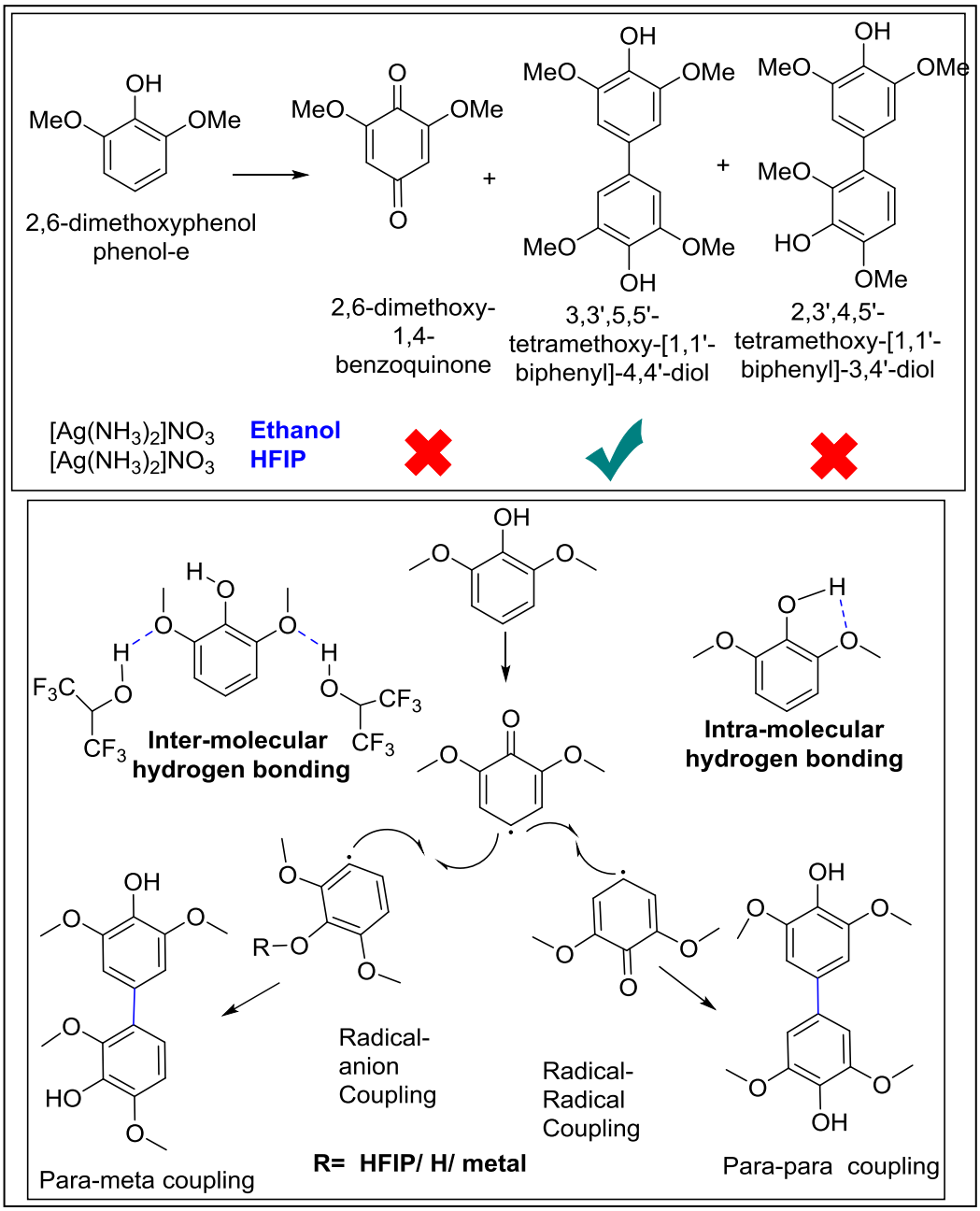

*where Coupling reaction of phenol-e in HFIP solvent results in the *para-meta* coupled product instead of *para-para* coupling due to intermolecular hydrogen bonding instead of interamolecular this results in a difference in nucleophilicity of phenol.

Furthermore, this study led us to pose a question, **"Is it possible to observe chemo-selectivity by any other mechanism**?"

For this question, we stumbled upon one curious experiment- when modified Tollens reaction for Cross-coupling in borosilicate glass test tube was carried in an Eppendorf tube, silver rather than the formation of mirror stops at the aggregated stage and floated on the solution. This prompted us to write these observations in the following three equation forms.

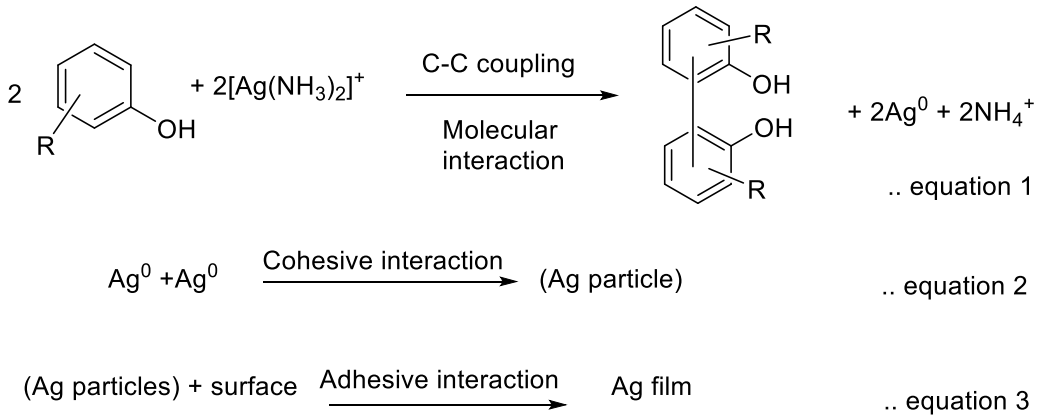

In the Tollens' reaction, phenols convert to bi-phenols, and Ag(*I*) reduces to Ag^0 and subsequently to a silver mirror. The oxidation, as shown by equation 1, happens due to molecular-level interaction while equations 2 and 3 show macroscopic level interactions. Equation 2 shows the aggregation or cohesive behavior of Ag^0 to form $Ag_{particle}$. Equation 3 shows adhesion of Ag particles on the surface, macroscopic behavior, and is distinctly different from atomic level absorbtion/adsorption. The macroscopic reaction, cohesive interaction between Ag^0-$Ag^{0,}$ and adhesive interaction of $Ag_{particles}$ with surface ultimately result in film formation on the test tube wall.[34,36,37]

The cross-coupling reaction of phenol-c with e by varying vessel surface

Scheme S3.3.9: Cross-coupling Reaction of Phenol-c with e by varying vessel surfaces

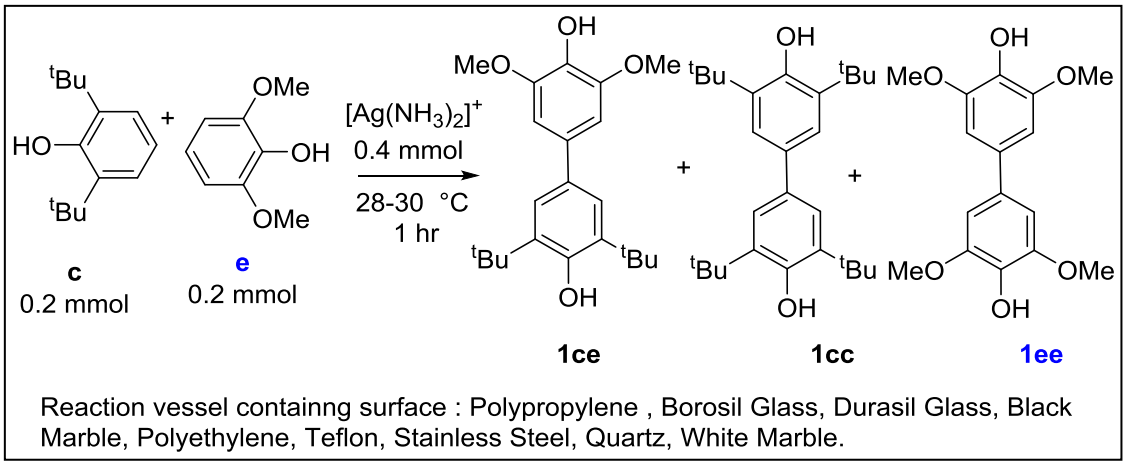

Phenol-c with e were chosen, and cross-coupling reactions were attempted, without 'addition' of any extra-reagent, but by only changing the surface of the reaction vessel, as shown in scheme S3.3.9. (Refer to section 3.5.7 for a detailed experimental procedure, where appropriate precautions are taken to correlate surfaces)To our surprise, the vast difference in the yield of cross-coupled products was observed, as shown in Figure 3.3.5. The yield of 1ce was varied from about 10% to 70% with distinct changes in silver formation are tabulated in Table T3.2. The homo-coupling products were formed during all the reactions. Plastic surface directed major cross-coupled products, whereas teflon surface offered major homo-coupled products.[39] Under the same reaction condition, the cross-coupling reaction was completed

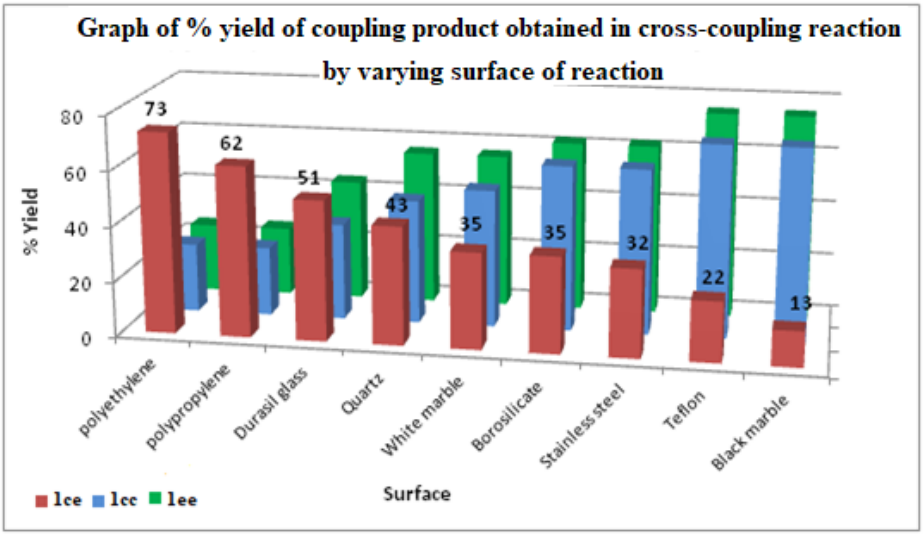

Figure F3.3.5 % yield of coupling products 1ce, 1cc and 1ee verses surfaces

The cross-coupling reaction of phenol-c with e by varying vessel surface

Scheme S3.3.9: Cross-coupling Reaction of Phenol-c with e by varying vessel surfaces

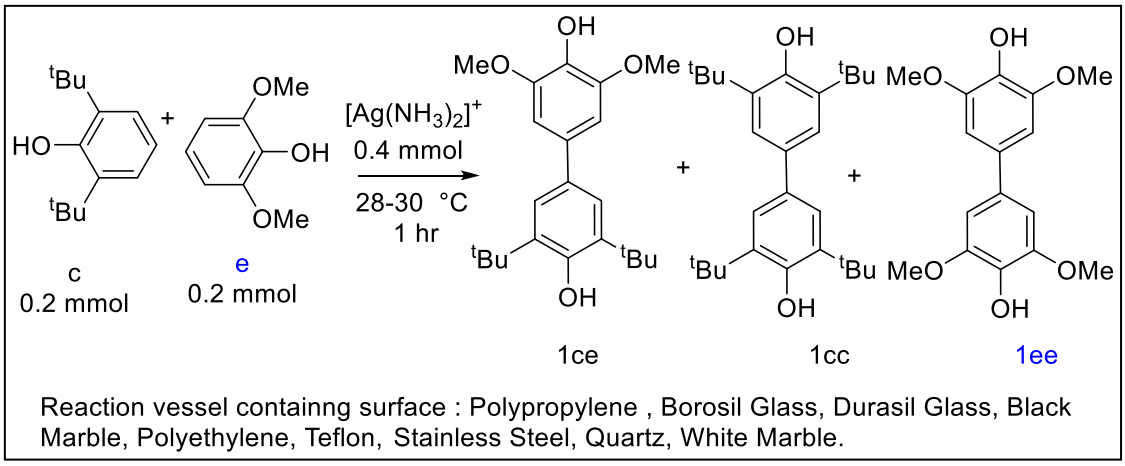

Phenol-c with e were chosen, and cross-coupling reactions were attempted, without 'addition' of any extra-reagent, but by only changing the surface of the reaction vessel, as shown in scheme S3.3.9. (Refer to section 3.5.7 for a detailed experimental procedure, where appropriate precautions are taken to correlate surfaces)To our surprise, the vast difference in the yield of cross-coupled products was observed, as shown in Figure 3.3.5. The yield of 1ce was varied from about 10% to 70% with distinct changes in silver formation are tabulated in Table T3.2. The homo-coupling products were formed during all the reactions. Plastic surface directed major cross-coupled products, whereas teflon surface offered major homo-coupled products.[39] Under the same reaction condition, the cross-coupling reaction was completed

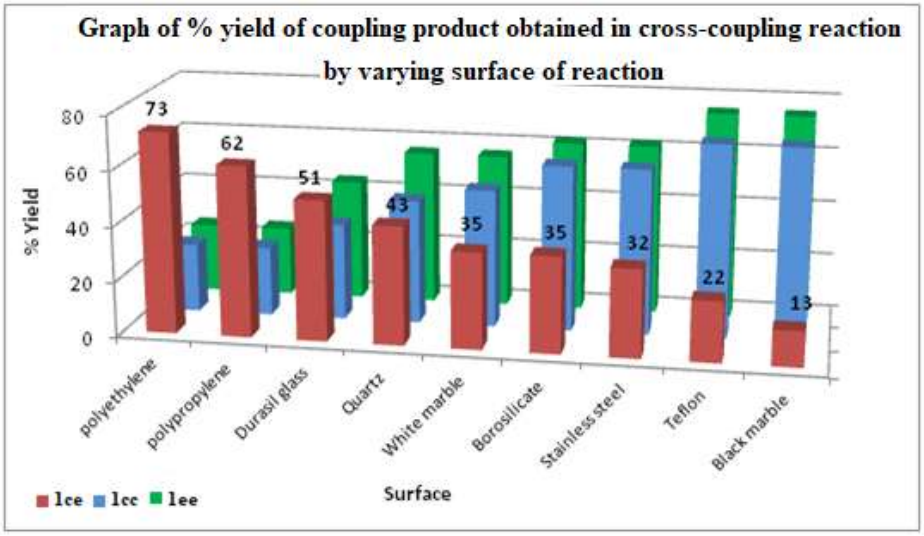

Figure F3.3.5 % yield of coupling products 1ce, 1cc and 1ee verses surfaces

faster (3-5 min) than corresponding homo-coupling reactions (15-30 min).

Table T3.2: C-C oxidative cross-coupling of c with e by varying surface*

No.	Surface	Surface area Used In cm^2	% yield of cross-coupled products on repeated experiments	Cross-coupled product yield in %	Homo-coupled products yield in %		Coupling selectivity	Time in min	Nature of Silver formed in the reaction
				1ce	1cc	1ee			
		(I)	(II)	(III)	(IV)	(V)	(VI)	(VII)	(IIX)
1	Polyethylene	10-20	70-80	73	25	25	cross	4-5	Fine Particles
2	Polypropylene	8	60-65	62	25	25	cross	5-6	Particles
3	Durasil glass	8	50-60	51	35	44	cross	5-7	Film
4	Quartz	8	40-45	43	45	56	-	10-15	Film+ Particles
5	White marble	10	30-35	35	50	56	-	5-10	Film+ particles
6	Borosilicate	8	30-35	35	60	62	-	4-5	Film
7	Stainless steel	8	25-30	32	60	62	-	10-15	Particles
8	Teflon	10	20-25	22	70	75	Homo	5-7	Film+ Particles

*where, (I) surface area of vessel surface contacting reaction mixture; % yield of isolated products calculated: (III)-(IV) based on c, and (V) phenol-e; (II) the 1ce formed is shown in the range obtained from repeated experiments; (VI) selectivity observed; (VII) time required for complete conversion; (IIX) silver formed in the reaction observed optically

The temperature, time, quality, quantity of reagents, addition, and order for mixing were kept constant for maintaining uniformity of the reaction conditions. The experiments were repeated more than five times to observe constancy in the observed results.

Analysis of Silver particles

We propose, aggregation of silver (Ag^0) on the macroscopic surface remained a key aspect of product formation's selectivity. These silver particles were isolated from reaction mixtures and analyzed using an optical microscope (with 8X-zoom power in reflection and transmission mode). The images obtained from optical microscopy of silver particles show dissimilar morphologies, but not with clarity, as shown in Figure F3.3.6.

Figure F3.3.6: Optical Microscopic images in transmission and reflection mode of silver obtained from C-C oxidative cross-coupling of phenol-c with e carried out in the different surface

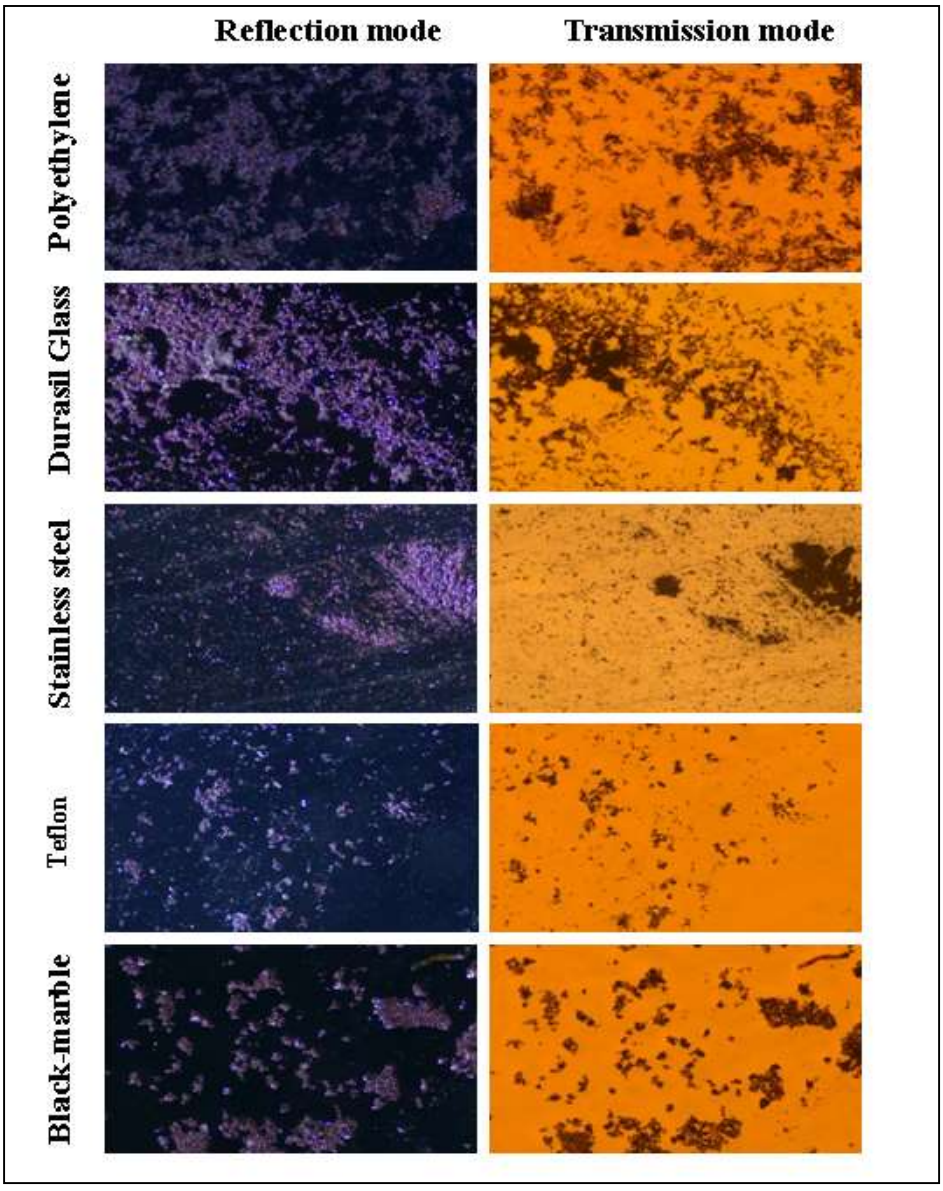

Figure F3.3.7: FE-SEM images of silver obtained from C-C oxidative cross-coupling reaction of phenol-c with e carried out in teflon surface

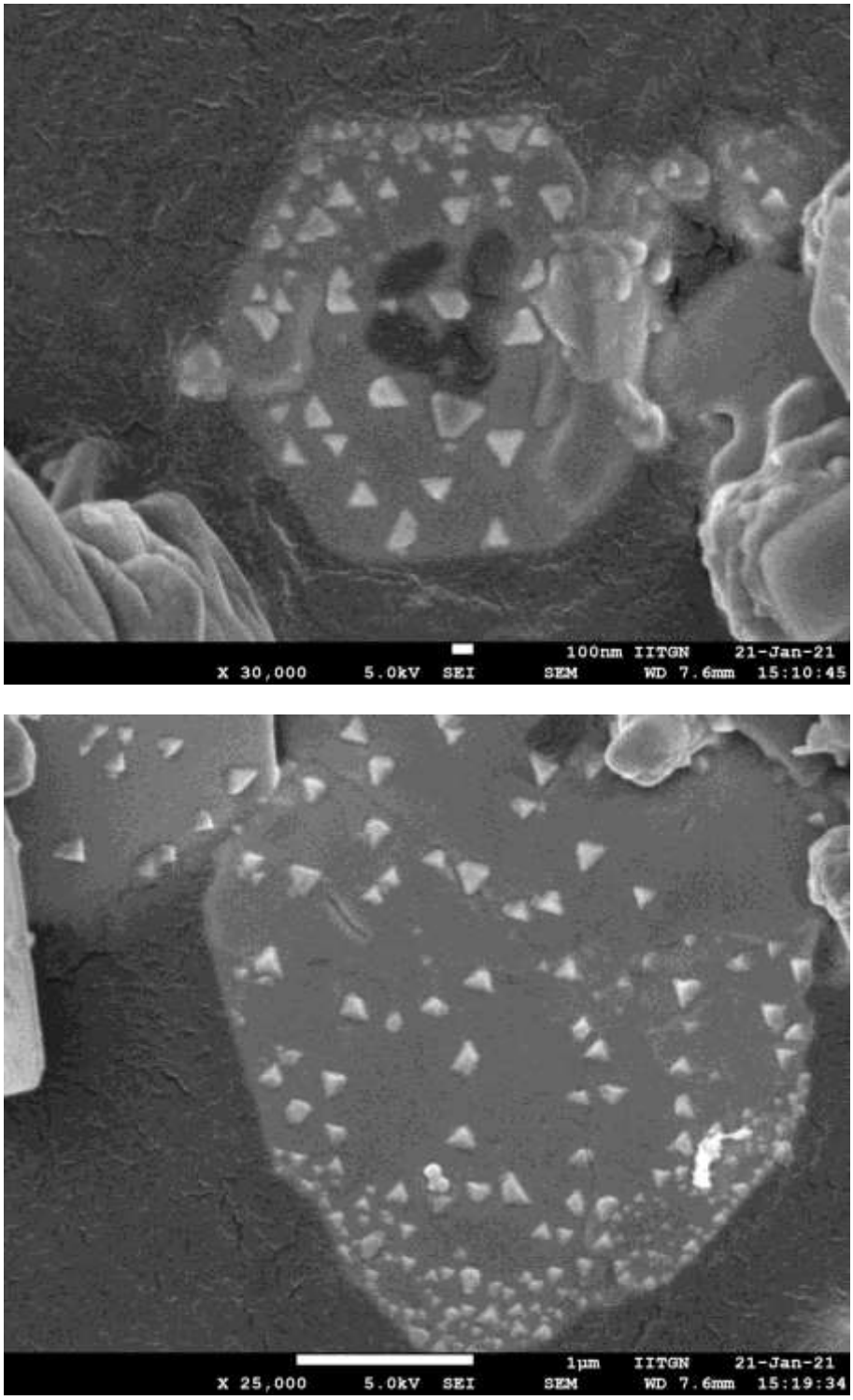

Figure F3.3.8: FE-SEM images of Silver obtained from C-C oxidative cross-coupling reaction of phenol-c with e carried out in polypropylene surface

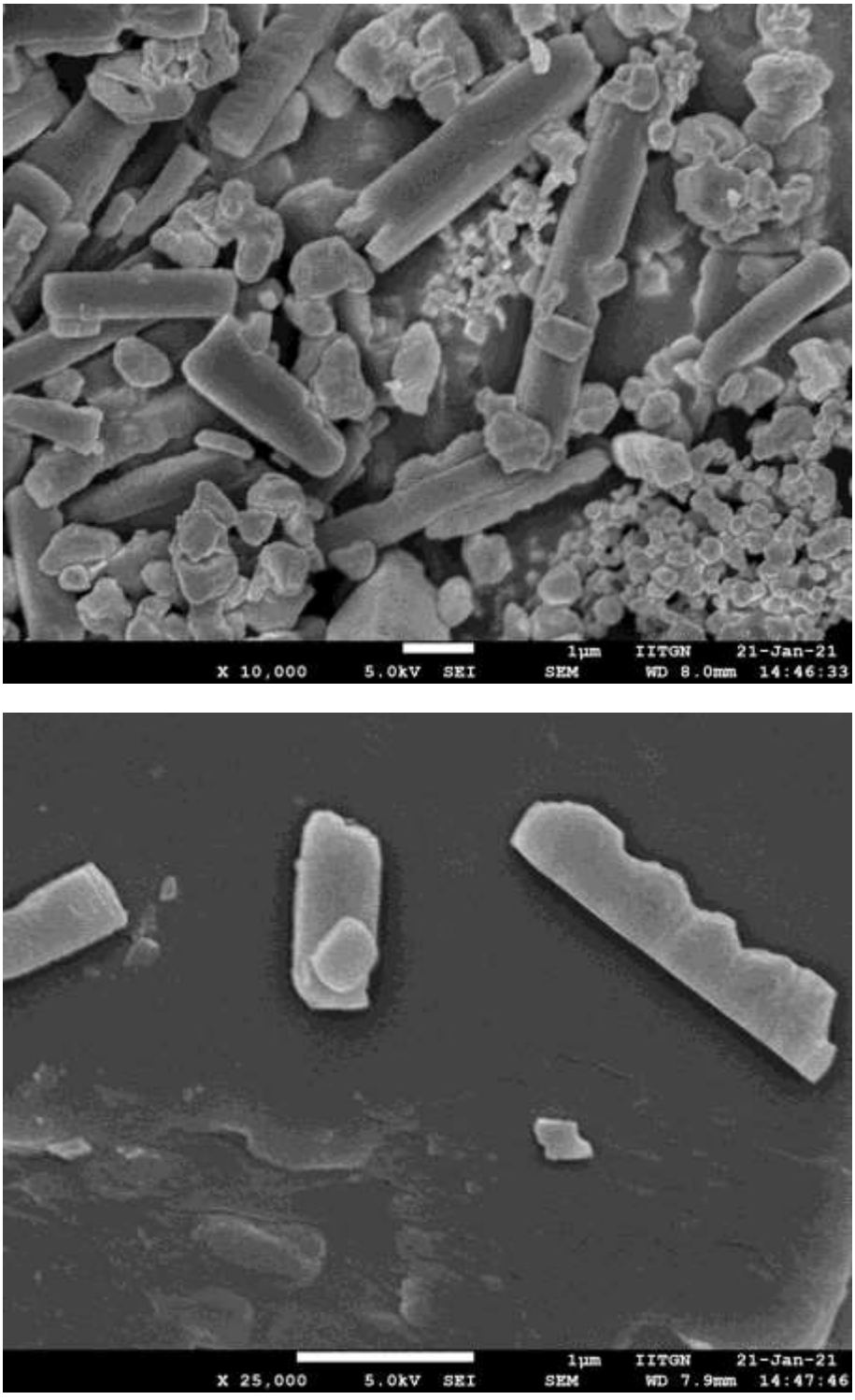

The nano-crystalline nature of silver particles was clearly observed in analyzing silver particles obtained from polypropylene and teflon surfaces using field emission scanning electron microscopy analysis (FE-SEM). The silver obtained from the teflon surface was of uniform truncated triangular shape with uniform base-lengths around 250 nm, as shown in Figure F3.3.7. The silver particles obtained from cross-coupling reaction of phenol-c with e in teflon surface were of two types, one with a cubic shaped with a width around 500 nm, and the other with rod-shaped having a width around 500 nm and varying lengths between 5-6 µm, as shown in Figure F3.3.8.

Figure F3.3.9: P-XRD data of silver particles obtained from C-C oxidative cross-coupling reaction of phenol-c with e carried out in Teflon Surface.

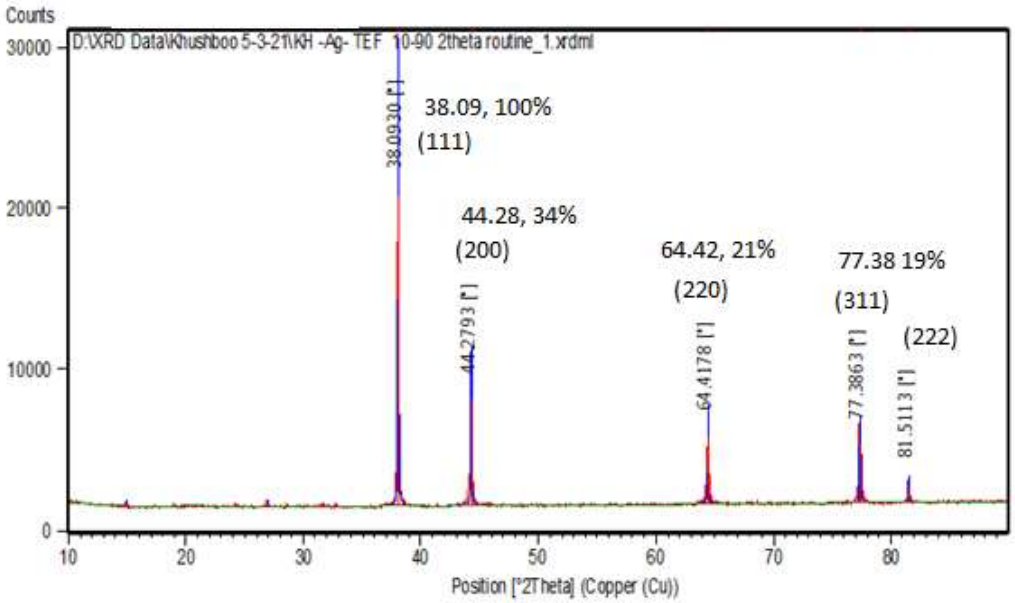

Pos.[°2Th.]	Height [cts]	FWHMLeft[°2Th.]	d-spacing [Å]	Area[cts*°2Th.]	Rel.Int [%]
14.9148	243.06	0.0630	5.93499	22.65	1.23
26.9369	258.28	0.1260	3.30728	48.14	1.31
31.6091	127.01	0.3149	2.82827	59.18	0.64
32.7523	165.48	0.0945	2.73212	23.13	0.84
38.0930	19761.96	0.0960	2.36045	3794.30	100.00
44.2793	6812.83	0.1056	2.04396	1438.87	34.47
64.4178	4252.21	0.0768	1.44519	653.14	21.52
77.3863	3694.81	0.0960	1.23218	709.40	18.70
81.5113	1172.48	0.1152	1.17993	270.14	5.93

Figure F3.3.10: P-XRD data of silver particles obtained from cross-coupling reaction carried out in polypropylene surface.

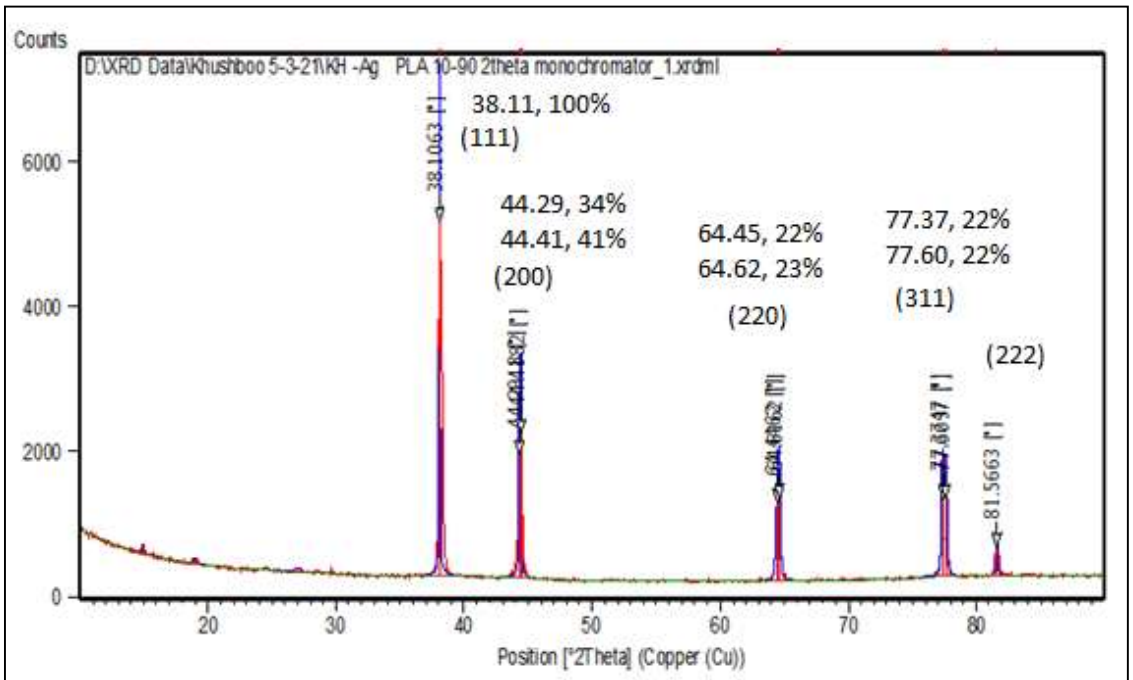

Pos.[°2Th.]	Height [cts]	FWHMLeft[°2Th.]	d-spacing [Å]	Area[cts*°2Th.]	Rel.Int [%
14.9412	157.95	0.1004	5.92458	23.46	3.17
18.9532	59.27	0.4015	4.67854	35.21	1.19
26.9767	82.88	0.3346	3.30249	41.03	1.66
38.1063	4986.60	0.1020	2.35966	1017.27	100.00
44.2918	1718.61	0.1020	2.04342	350.60	34.46
44.4182	2025.01	0.1020	2.03789	413.10	40.61
64.4462	1091.79	0.1632	1.44462	356.36	21.89
64.6162	1146.22	0.1632	1.44123	374.13	22.99
77.3747	1103.68	0.1632	1.23234	360.24	22.13
77.6037	1101.03	0.2040	1.22927	449.22	22.08
81.5663	393.41	0.1632	1.17927	128.41	7.89

The P-XRD of silver particles obtained from teflon and polypropylene surfaces were larger similar, and are presented in Figures F3.3.9 and F3.3.10. The reflections at 2θ of 38.1º, 44.3º, 64.5º, 77.5º, and 81.5º can be indexed to the (111), (200), (220), (311), and (222) reflections of the Face centered cubic-lattice crystalline system. Due to the densely packed layer, the (111) reflection was observed strongest. Silver obtained from the teflon surface showed a distinct difference due to the presence of double reflections with almost 1:1 intensities at 2θ of 44.29º-44.41º, 64.45º-64.62º, and 77.37º-77.60º. We are presently understanding its origin.

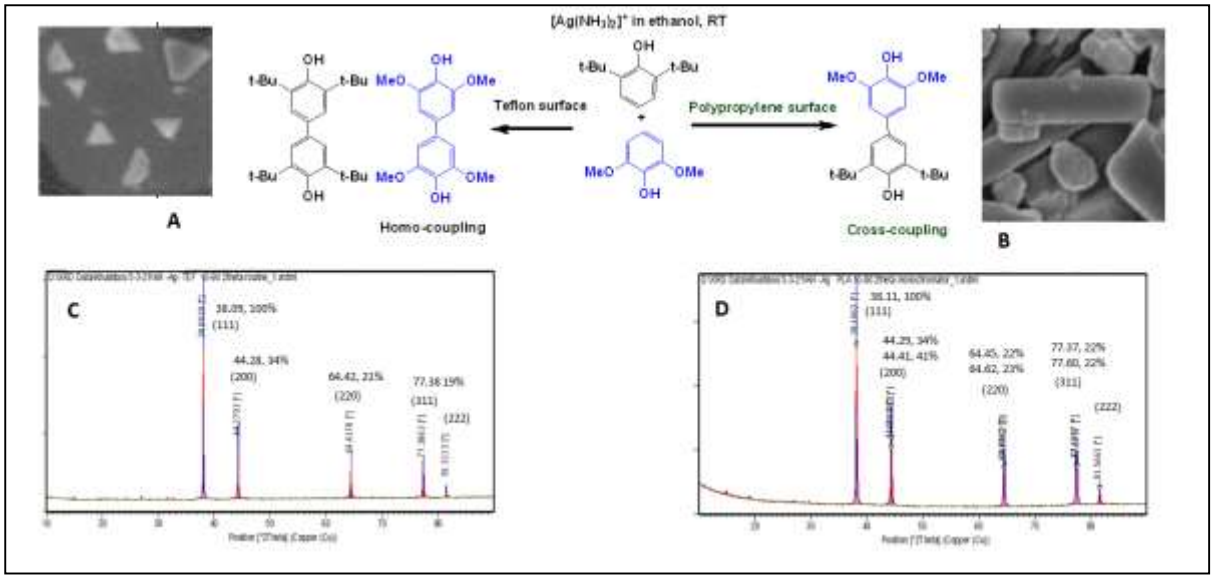

Figure F3.3.11: C-C oxidative cross coupling of phenol-c and e in teflon and polypropylene surfaces: FE-SEM images of silver obtained from teflon surface (A) and Plastic surface (B) : P-XRD spectra of silver obtained from teflon surface (C) and Plastic surface (D)

In short, these results reveal the active role of concurrent growth of silver particles and chemo-selectivity, as shown in Figure F3.3.11. Traditionally, the type and concentration of the capping agent and/or modifier control the size and shape of the silver particles during growth in the reaction, due to molecular-level controlled agglomeration of silver particles, with Ag-Ag cohesive interaction.[36] This means, in the Tollens' reaction, Ag particles experience cohesive interaction among themselves on one hand and adhesive interaction with the surface, where the latter leads to thin-film or mirror formation on the walls of a test tube. Thus, one can say that the non-adhesive (or repulsive) force of the surface can restrict the growth of Ag^0 to silver particles, which ultimately drives oxidative coupling reactions.

Mechanism

The above results helped us to propose a hypothesis based on Cohesion-Adhesion interactions of Ag^0 to $Ag_{particle}$ to Ag-film and hence selectivity in C-C oxidative cross-coupling, as depicted in Figure F3.3.12. The reaction gets controlled by two dominant interactions - molecular interaction and macroscopic interaction. The molecular interactions are (I-A) exchange of electrons between $[Ag(NH_3)_2]^+$ and phenol; and (I-B) carbon-carbon bond formation (interaction between two phenol molecules) And two macroscopic interactions are (II-A) Ag^0-Ag^0 cohesion to form $Ag_{particle}$ and (II-B) ($Ag_{particle}$)-surface adhesion. We assume, "the surface affects ($Ag_{particle}$)-surface adhesive interaction and hence direct Ag-Ag cohesive interaction, which in turn influence chemo-selectivity in oxidative product formation." Three probable dynamics/mechanisms are shown in Figure F3.3.12 showing the progress of the reaction (left- initial stage to right-final stage), in accordance with three equations 1-3 (on page 90).: (A) only molecular interactions ; (B) Ag^0-Ag^0 cohesion to form $Ag_{particle}$; (C*)* $Ag_{particle}$-surface adhesion interaction and formation of a thin film.

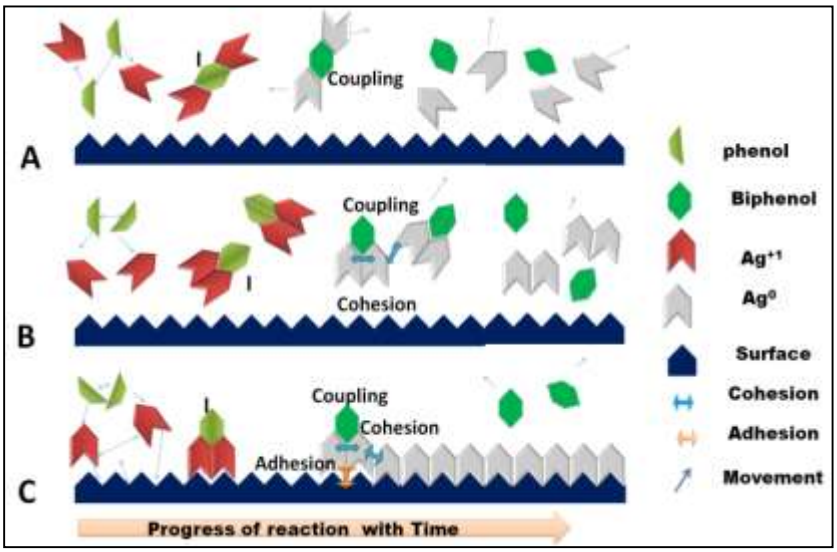

Figure F3.3.12**:** Probable reaction dynamics

UNSUCCESSFUL ATTEMPTS

The C-C oxidative cross-coupling reaction of phenol-h with e by varying vessel surface

Scheme S3.3.10: C-C oxidative cross-coupling reaction of Phenol-e with h in different surfaces

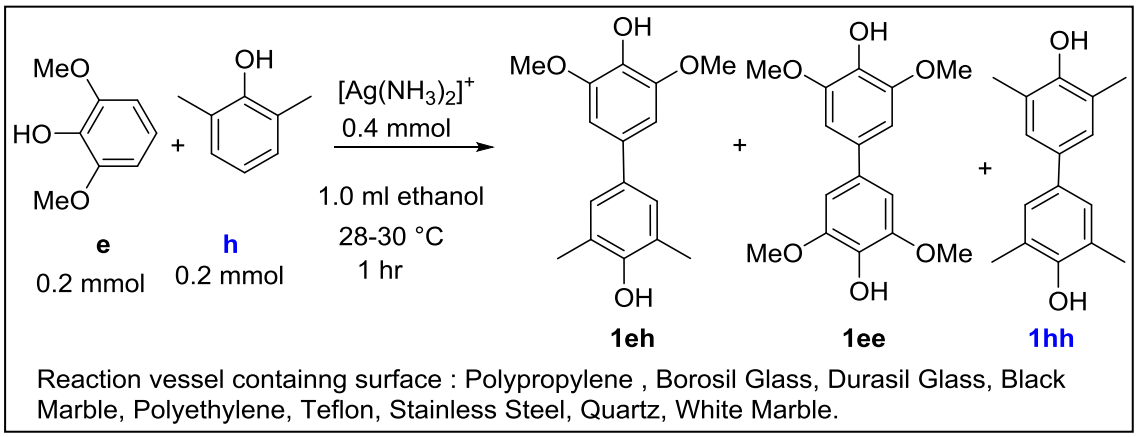

Table T3.3 C-C oxidative cross-coupling of phenol-e with h by varying reaction vessel surface*

No.	Surface	Surface area Used in cm^2	Cross-coupled product 1eh yield in %	Homo-coupled product yield in % 1ee
1	Polyethylene	10-20	26	36
2	Polypropylene	8	19	16
3	Durasil glass	8	22	28
4	Quartz	8	22	21
5	White marble	10	28	36
6	Borosilicate	8	18	24
7	Stainless steel	8	18	36
8	Teflon	10	20	21

* isolated product yields are shown in %, and were calculated based on phenol-e

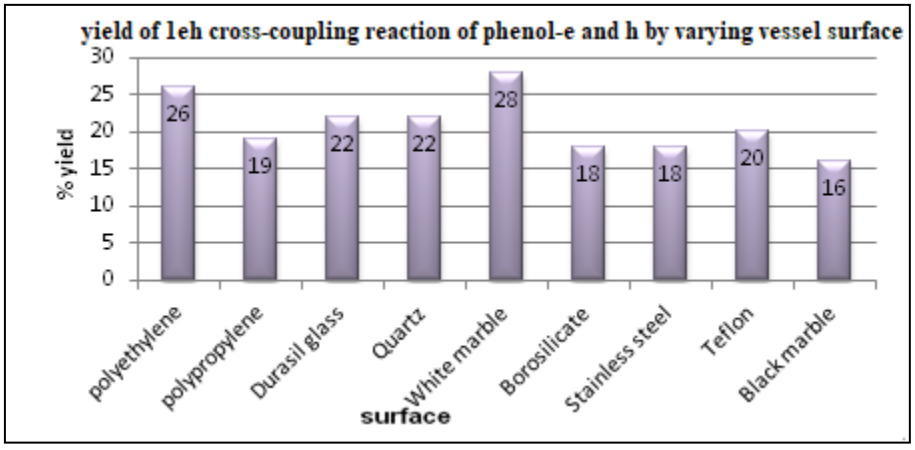

Figure F3.3.13: % Yield of 1eh obtained verses used surfaces of the vessel for cross-coupling reaction of phenol-e with h

To extend the scope of this methodology cross-coupling reaction between phenol-c and h was attempted in different surfaces, as shown in scheme S3.3.10. (Refer to section 3.5.7 for detailed experimental procedure). Complete results along with reaction conditions were shown in table T3.3 and graphically presented in Figure 3.3.13. These experiments have been repeated a minimum of five times, and a minor selective cross-coupling product was obtained all the time. Polyethylene and white marble surface directed major cross-coupled product 1eh, while borosilicate and steel surface gave major homo-coupled product 1ee. The difference in the yield of cross-coupling product 1eh by changing surface was about 12%, which was not a remarkable difference. The non-observation of selectivity can be correlated to over oxidized multiple byproduct formation.

The C-C oxidative cross-coupling reaction of phenol-c with e by varying vessel surface

Scheme S3.3.11: C-C oxidative cross-coupling of Phenol-c with h by varying vessel surface

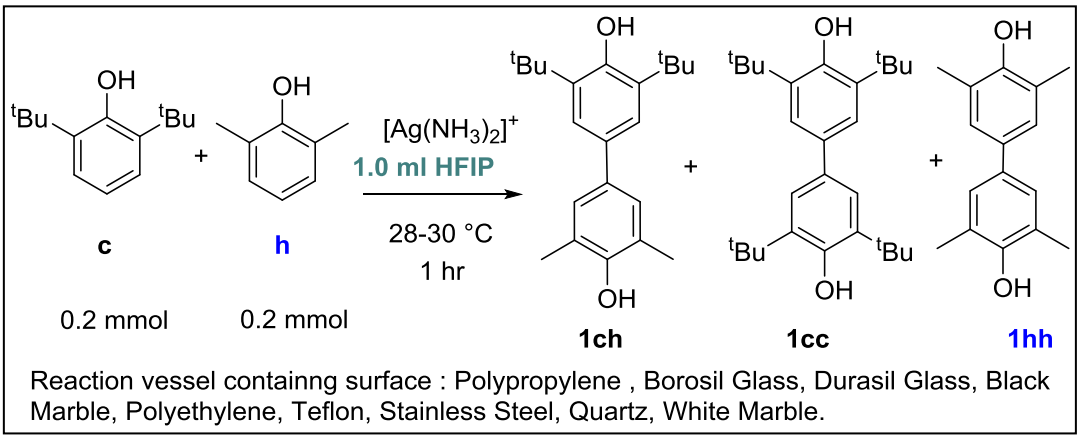

The reaction of phenol-c with h was also carried out on these surfaces using silver ammine complex, as shown in scheme S3.3.11. Although all these reactions resulted in homo-coupling product formations even after changing surface.

Role of the surface area on cross-coupling reaction

The cross-coupling reaction of Phenol-c with e was attempted in different sizes of vessels (different surface areas), but with the same surface (borosilicate glass/polypropylene/durasil glass), as shown in table T3.4. (Refer to section 3.5.8 for a detailed experimental procedure, where different shapes and sizes of vessels are discussed). The consistency in the cross-coupling yield (29-35%) was obtained, using borosilicate glass (Table T3.4 1 to 6). This reaction was again repeated with polypropylene (Table T3.4 7 to 11) and durasil glass surface containing vessels (Table T3.4 12 to 17), but with no trend for selectivity.

Table T3.4: Effect of size of vessel used for C-C oxidative cross-coupling reaction of phenol-c with e *

No.	The surface area in cm^2	Surface	Cross-coupled product in % **1ce**	Homo-coupled products in %	
				1cc	**1ee**
		Borosilicate glass			
1	20	2.0 ml graduated pipette	**29**	60	60
2	8	5.0 ml test-tube	**34**	55	52
3	8	10.0 ml test tube	**35**	56	55
4	10	5.0 ml beaker	**29**	60	58
5	10	10.0 ml beaker	**29**	63	58
6	12	25.0 ml beaker	**31**	58	57
		Plastic Polypropylene			
7	8	2.0 ml eppendorf	**62**	25	25
8	8	5.0 ml beaker	**58**	26	23
9	10	10.0 ml beaker	**63**	22	22
10	12	25.0 ml beaker	**65**	23	25
11	12	50.0 ml beaker	**60**	25	22
		Durasil glass			
12	8	5.0 ml test-tube	**48**	44	35
13	8	10.0 ml test tube	**50**	42	32
14	10	5.0 ml beaker	**52**	40	36
15	10	10.0 ml beaker	**50**	42	38
16	12	25.0 ml beaker	**53**	42	36
17	20	5.0 ml watch glass	**48**	43	35

* the yield is shown in % of isolated product; 1ce and 1cc calculated based on c: 1ee calculated based on e.

The coupling reaction of 2,6-dimethoxyphenol (phenol-e) by varying vessel surface using 1) silver ammine complex and ethanol solvent, 2) by using silver ammine complex and HFIP solvent, 3) by using ferric chloride reagent

Scheme S3.3.12: Effect of surface on C-C oxidative coupling of Phenol-e using ferric chloride and silver ammine complex

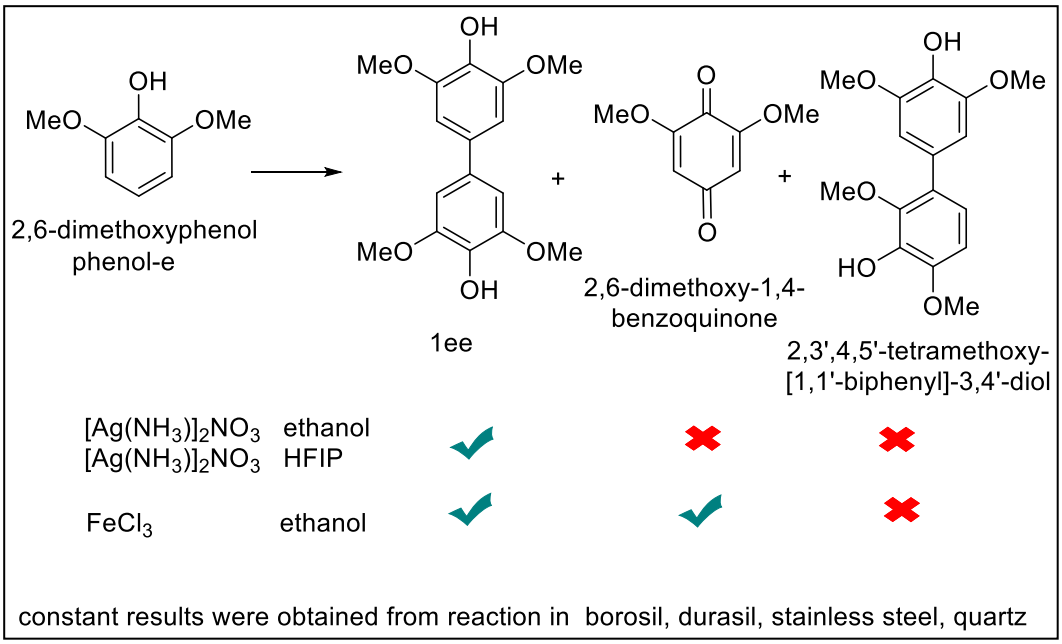

To extend our understanding of $[Ag(NH_3)_2]^+$ and surface for the observed chemo-selectivity C-C oxidative coupling of phenol-e was attempted using ferric chloride in different (borosilicate glass, durasil glass, quartz, or stainless steel) surfaces, as shown in the scheme S3.3.12. (Refer to section 3.5.9 for detailed experimental procedure). However, this reaction could not result in *meta-para* coupling product formation. The possibility of surface-directed chemo-selectivity due to change in radical-radical or radical-anion coupling mechanisms was not observed.

3.4 Summary

In summary, the silver ammine complex, modified Tollens' reagent, was studied for effective C-C oxidative cross-coupling reactions.

- Silver ammine complex can act as an efficient and mild reagent for carrying out the C-C oxidative cross-coupling reaction of phenols and naphthol derivatives.
- Total six (6) C-C cross-coupled products were obtained quantitatively with moderate yield (up to 58%) and characterized using mass-spectrometry, FT-NMR (^{1}H and ^{13}C), and FT-IR spectroscopy analysis. All data were consistent with the literature.
- Based on oxidation potential difference, E_{ox} and $N_{o,}$ phenol-c, e, and h were selected for a mechanistic study. Various strategies were used to increase cross-coupling efficiency and optimize reaction conditions. The chemo-selectivity was not achieved using HFIP solvent; based on these studies, a radical-radical coupling mechanism was proposed for the reaction.
- The yield of cross-coupled product 1ac can be increased from 15% to 70% by only changing the surface of the reaction vessel from the teflon to borosilicate glass to polyethylene material.
- The silver film and/or particles formed during the C-C oxidative coupling reaction were analyzed by P-XRD analysis, optical microscopy, and FE-SEM. Nano-crystalline structures having Face-centered cubic arrangement having different morphology from triangular pallets to cubical-rod shape morphology of silver on using Teflon to polypropylene surface, and formation of homo- to cross-coupling selectivity revealed surface-assisted chemo-selectivity.

In short, the present investigation revealed an active role of macroscopic interaction in 'manipulating' molecular level interactions and hence the product formation. A new synthetic scheme is designed and discussed in chapter 4 to support the proposed hypothesis.

3.5 Experimental

3.5.1 Materials

Silver nitrate was purchased from Sigma-Aldrich of 99.9999% purity. All other chemicals used were of analytical grade quality, purchased commercially from Sigma-Aldrich, Alfa Aesar, TCI, or Avra chemicals, and used without further purification. Absolute alcohol (99.6 % v/v) was acquired from the Maharaja Sayajirao University of Baroda and was used without further purification. Distilled water was used in preparing the sample solution, which was double-distilled de-ionized in an all-glass distillation setup (specific conductivity of less than 10 μS cm^{-1} at 30°C). All other solvents were purchased commercially from local sources.

3.5.2 Methods and Characterization

- These reactions were conducted in the presence of air. (mentioned if not)
- The reactions have been repeated a minimum of five times. Yields of reactions are presented in percentage, which is an average of results of repeated experiments. Maximum ±1.5% difference was observed in isolated yield of organic compounds, a determined error.
- Thin-layer chromatography was performed using a TLC 60 F254 plate of silica gel of 60 mesh coated on an aluminum plate purchased from Merck.
- The vessels used in the reaction were pre-cleaned and rinsed with dilute HNO_3 and de-ionized water. Most of the reactions were performed in an oven-dried, custom-made glass test tube of 10 ml. It is mentioned if another vessel is used.
- The products were purified by column chromatography using Fluka chromatographic silica gel (40-60 μm).
- Proton nuclear magnetic resonance (^{1}H NMR) spectra and carbon nuclear magnetic resonance (^{13}C NMR) spectra were recorded on Advanced Bruker-400 NMR spectrophotometers with $CDCl_3$. Chemical shifts for protons are reported in parts per million downfield from *tetra*methylsilane, and coupling constants are shown in Hertz (Hz). Chemical shift multiplicity as s = singlet, d = doublet, t = triplet, q = quartet, and m = *multiplet.*
- MS data were obtained from electron spray ionization mass spectral measurement (ESI-MS), which were performed using ESI-mass Applied Biosystem API 2000 mass spectrometer.

- Infrared spectra (400–4000 cm^{-1}) were recorded on α-Bruker FTIR with samples prepared as KBr pallets.
- P-XRD pattern of silver particles s was recorded with X'pert Pan Analytical Powder diffractometer, by using the following instrument parameters: X-ray source: Cu Kα radiation (λ =0.154060 nm); Current 40 mA, Voltage:40kV; 2Θ value from 10° to 90° in continuous scanning mode at 25.00°C.
- The microscopic FE-SEM images were recorded using Field Emission Scanning Electron Microscope JSM7600F (Jeol) instrument.

3.5.3 General scheme for C-C oxidative cross-coupling reaction of phenol derivatives

0.2 mmol of phenol-1 and 0.2 mmol of phenol-2 (a-i) were mixed and dissolved in absolute ethanol (1.0 ml) to add to the vessel (borosilicate). Silver ammine complex was prepared by dissolving the silver nitrate (0.0680 g, 0.4 mmol) in a liquor ammonia (0.2 ml) solution. The silver-ammonia complex solution was added into the solution of phenol and stirred using a magnetic stirrer. The product formation was monitored using thin-layer chromatography. The products were extracted and purified using column chromatography. The cross-coupled products were characterized by FT-NMR (^{1}H and ^{13}C) spectroscopy (Figures F3.6.1 to F3.6.6), FT-IR spectroscopy (Figures F3.6.14 to F3.19), and mass spectrometry analysis (Figures F3.6.7 to F3.13), as shown in section 3.5.17.

3.5.3.1 General procedure for the effect of a stoichiometric amount of phenol

The phenol solution was prepared by dissolving Phenol-c (0.0412 g, 0.2 mmol) and phenol-e (1.0/ 1.2/ 1.5/ 0.8 mole Equiv.) in 1.0 ml absolute ethanol. The silver ammine complex solution was prepared by dissolving the silver nitrate (0.0680 g, 0.4 mmol) in a liquor ammonia (0.2 ml) solution. The phenol solution was added to the vessel (borosilicate) followed by the addition of silver-ammonia complex solution and stirred at 30 °C using a magnetic stirrer for 60 minutes. The product was extracted using ethyl acetate and (5.0 ml) dichloromethane (5.0 ml) in 0.5 ml fractions of each. All these solvents were dried over Na_2SO_4 and evaporated. The residue was purified using column chromatography on silica gel to yield the products.

3.5.3.2 General procedure for the effect of reaction temperature

Phenol-e (0.031 g, 0.2 mmol) and phenol-c (0.041 g, 0.2 mmol) were mixed, and dissolved in 1.0 ml absolute ethanol and added to vessel (borosilicate). The silver ammine complex

solution was prepared by dissolving the silver nitrate (0.0680 g, 0.4 mmol) in a liquor ammonia (0.2 ml) solution. The silver-ammonia complex solution was added to the solution of phenol. These reaction mixtures were kept at 10°C, 30°C, or 70°C temperature in a chilled water bath, at room temperature water bath, in pre-heated water bath respectively until maximum conversion. The products were isolated from the reaction mixture and purified column chromatographically.

3.5.3.3 General procedure for the effect of dilution

Phenol-e (0.0308 g, 0.2 mmol) and phenol-c (0.0412 g, 0.2 mmol) were mixed, and dissolved in absolute ethanol (0.4, 2.0 or 10 ml) and added to vessel (borosilicate). The silver ammine complex solution was prepared by dissolving the silver nitrate (0.0680 g, 0.4 mmol) in a liquor ammonia (0.2 ml) solution. The silver-ammonia complex solution was added to the phenol solution and stirred at room temperature using a magnetic stirrer, until maximum conversion. Extraction was done after drying all solvent using a total of 5 ml MDC and 5 ml ethyl acetate, used in 0.5 ml fractions. The products were purified column chromatographically.

3.5.4 General procedure for C-C oxidative cross-coupling in HFIP solvent

Phenol-1 (0.2 mmol) and phenol-2 (0.2 mmol) (phenol-c/e/h) were mixed, and added to a closed glass test tube of 10 ml. 1.0 ml HFIP was added to the phenol-containing vessel and stirred using a glass needle for 60 minutes at 30°C. The silver-ammonia complex solution was prepared by dissolving the silver nitrate (0.0680 g, 0.4 mmol) in a liquor ammonia (0.4 ml) solution. The organics were extracted from the reaction mixture using DCM and ethyl acetate solvent. The products were purified column chromatographically.

3.5.5 General procedure for C-C oxidative cross-coupling of phenol-e in HFIP solvent

Phenol-e (0.0308 g, 0.2 mmol) was dissolved in 1.0 ml of HFIP in a closed glass test tube and stirred using a glass needle for 60 minutes at 30°C. The silver-ammonia complex solution was prepared by dissolving the silver nitrate (0.0340 mg, 0.2 mmol) in 0.2 ml liquor ammonia. This silver ammine complex was added into phenol solution and stirred for 30 to 60 minutes. The organic products were isolated and purified using column chromatography.

3.5.6 General procedure for C-C oxidative cross-coupling in presence of hydrogen peroxide

Phenol-c (0.0412 g, 0.2 mmol) and phenol-e (0.0308 g, 0.2 mmol) were mixed, and dissolved in 1.0 ml ethanol. 0.5 ml hydrogen peroxide solution was added to the phenol and stirred using a glass needle for 60 minutes at room temperature. Silver ammine complex, prepared by dissolving the silver nitrate (0.0680 g, 0.4 mmol) in liquor ammonia (0.4 ml) solution, was added into phenol solution and stirred for 30 minutes. Extraction was done using dichloromethane and ethyl acetate (4 ml of each) to the mixture for isolation of the organic products from silver. Finally, all these solvents were dried, and the resultant residue was subjected to column chromatography for the purification of products.

3.5.7 General procedure for C-C oxidative cross-coupling reaction by changing surface of the vassel

Cross-coupling reactions were carried out in parallel on different surfaces using an identical procedure to compare the effect of surface on the reaction product formation; thus, all the time, all reactions were carried out in stipulated time to achieve identical reaction conditions. Furthermore, to maintain uniformity in all reactions, standard reagents were prepared in bulk used that quantitatively.

Silver nitrate was dissolved into a liquor ammonia solution to prepare a standard silver ammine solution diluted in a standard volumetric flask. Both the Phenols were taken in the one-one mole equivalent and dissolved in absolute ethanol to prepare a standard phenol solution. Phenol solution was added to different containers having different surfaces material such as polyethylene, polypropylene, borosilicate glass, durasil glass, marble, Teflon, stainless steel, and quartz. After some time, the silver-ammonia complex solution was added into phenol solution and mixed at room temperature.

After a stipulated time, all organic compounds were extracted from crude using dichloromethane and ethyl acetate (5 ml of each). These extracts were collected and dried over a rota-evaporator and subjected to column chromatography. The column chromatography was carried out using 5.0 ml of silica as a stationary phase and ethyl acetate-hexane mixture as a mobile phase on the column of 2 cm diameter to obtain organic products.

3.5.7.1 General Procedure of C-C oxidative cross-coupling reaction of phenol-c and e by a changing surface of the vessel

Phenol-e (0.031g, 0.2mmol) and phenol-c (0.041 g, 0.2 mmol) mixture was dissolved in 0.4 absolute ethanol and added to the containers. After 2 minutes, the silver-ammonia complex solution was prepared by dissolving (0.0680 g, 0.4 mmol) in 0.2 ml liquor ammonia was added to the phenol solution. 0.6 ml of ethanol was added to the reaction mixtures and kept for 1 hr at 30°C after mixing by shaking the vessel for few seconds.

The organics were extracted from crude using dichloromethane and ethyl acetate (5 ml of each). These extracts were collected and dried over a rota-evaporator and subjected to column chromatography. The column chromatography was carried out using 5.0 ml of silica as a stationary phase and ethyl acetate-hexanes mixture as a mobile phase on the column of 2 cm diameter to obtain organic products. Washing of remaining crude was done with 1.0 ml of methanol and 1.0 ml water to obtain silver and dried in the oven at 70°C.

3.5.7.2 General Procedure of C-C oxidative cross-coupling reaction of phenol-e with phenol-h by a changing surface of the vessel

1.0 ml phenol solution containing a mixture of phenol-e (0.0308 g, 0.2 mmol) and phenol-h (0.0244 g, 0.2 mmol) in ethanol was added to the containers. After 2 minutes, the silver-ammonia complex solution was prepared by dissolving silver nitrate (0.0680 g, 0.4 mmol) in 0.2 ml liquor ammonia was added into phenol solution and kept at 30°C and kept for 1 hr after mixing by shaking the vessel for few seconds. The organic products were extracted from crude using a total of 5 ml MDC and 5 ml ethyl acetate solvents (used in 0.5 ml fractions). These extracts were collected and dried over a rota-evaporator. The resultant residue was purified using column chromatography.

3.5.7.3 General Procedure of C-C oxidative cross-coupling reaction of phenol-c with h by a changing surface of the vessel

1.0 ml of Phenol solution containing a mixture of phenol-h (0.0244 g, 0.2 mmol) and phenol-c (0.0412 g, 0.2 mmol) in ethanol was added to the containers. After 2 minutes, the silver-ammonia complex solution was prepared by dissolving silver nitrate (0.0680 gm, 0.4 mmol) in 0.2 ml liquor ammonia was added into phenol solution at 30°C and kept for 1 hr after mixing by shaking the vessel for few seconds. The organic products were extracted from

crude using a total of 5 ml MDC and 5 ml ethyl acetate solvents (used in 0.5 ml fractions). These extracts were collected and dried over a rota-evaporator. The resultant residue was purified using column chromatography.

3.5.8 General procedure for C-C oxidative cross-coupling reaction by changing the size of vessel surface

C-C oxidative cross-coupling of phenol-c and e were carried out using the procedure shown for experiment 5.5.4. Herein different containers were used having the same material of surface but different in shape and/or size as shown below.

- 2.0 ml graduated pipette, 5.0 ml test-tube, 10.0 ml test tube, 5.0 ml beaker, 10.0 ml beaker, 25.0 ml beaker were used as reaction vessels made up of borosilicate glass.
- 2.0 ml Eppendorf, 5.0 ml beaker, 10.0 ml beaker, 25.0 ml beaker, 50.0 ml were used as reaction vessels made up of polypropylene.
- 5.0 ml test-tube, 10.0 ml test tube, 5.0 ml beaker, 10.0 ml beaker, 25.0 ml beaker, and 5.0 ml concave watch glass were used as reaction vessels made up of durasil glass.

3.5.9 General procedure for C-C oxidative coupling of phenol-e using ferric chloride by varying surface

Ferric chloride (0.033 g, 0.20 mmol) was dissolved into 0.2 ml water to prepare the ferric chloride reagent. 1.0 ml of phenol-e (0.031 g, 0.2 mmol) solution in ethanol was added to the containers (having a surface of borosilicate, durasil, quartz, or stainless steel) at 30°C, and kept aside for 60 minutes.

3.5.10 Charactrization of product

All the organic products were known and identified by matching their melting point, FT-NMR (^{1}H and ^{13}C), FT-IR spectroscopic data, and mass spectrometric data with literature.

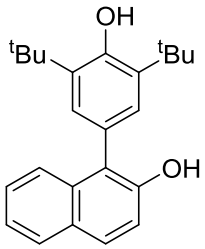

1-(4'-Hydroxy-3',5'-di-*tert*-butyl phenyl)-2-naphthol (1ac) was obtained by column chromatography on silica gel using ethyl acetate-hexanes : brown semi solid, up to 10% isolated column purified yield; ^{1}H NMR (400 MHz, $CDCl_3$, 291 K) δ 1.48 (18H, s), 5.32 (1H, broad, -OH), 5.39 (1H, broad, -OH), 7.19 (2H, s), 7.32-7.37(3H, m), 7.45 (1H, d, *J* = 8.4 Hz), 7.78-7.84 (2H, m); ^{13}C NMR (100 MHz, $CDCl_3$, 291 K) δ 30.4, 30.6, 117.2, 121.9, 123.2, 124.4, 124.9, 126.3, 127.6, 128.0, 128.9, 129.0, 133.7, 137.2, 150.4, 154.0; ESI-MS m/z: $[M]^{+1}$: 348.3 (molecular weight: 348.21 g/mol); FTIR 3299, 3223, 3058, 1628, 1601, 1508, 1482, 1359, 1251, 893, 847, 819, 740, 626 cm^{-1}.

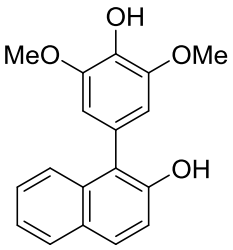

1-(4'-Hydroxy-3',5'-di-methoxy phenyl)-2-naphthol (1ae)[40] was obtained by column chromatography on silica gel using ethyl acetate-hexanes light brown solid; up to 8% isolated column purified yield ; mp: 163-165 °C ^{1}H NMR (400 MHz, $CDCl_3$, 291 K) δ 3.75 (6H, 2s), 6.43 (1H, d, *J* = 3.2), 6.61 (1H, d, *J* = 3.2), 7.26 (1H, d, *J* = 8.8), 7.32-7.37 (2H, m), 7.46-7.47(1H, m), 7.79-7.82 (2H, m); ^{13}C NMR (100 MHz, $CDCl_3$, 291 K) δ 55.9, 56.2, 106.3, 106.5, 116.6 , 117.9, 119.3, 123.5, 124.9, 126.7, 128.3, 129.3, 130.1, 133.1, 134.9, 148.3, 150.9; ESI-MS m/z: $[M-1]^{+1}$: 295.1 (molecular weight: 296.11 g/mol); FTIR (cm^{-1}) 3289, 3123, 2682, 1659, 1562, 1468, 1420, 1350, 1309, 1266, 1199, 1097, 825, 693, 550 cm^{-1}.

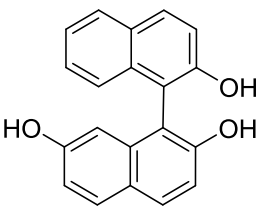

1,1'-binaphthyl-2,7,2'-triol (1ag)[41] was obtained by column chromatography on silica gel using ethyl acetate-hexanes : light grey semi solid; up to 16% isolated column purified yield; ^{1}H NMR (400 MHz, $CDCl_3$, 291 K) δ 4.83 (1H, broad, -OH), 5.00 (1H, broad, -OH), 5.09 (1H, broad, -OH), 6.37 (1H, d, *J* = 1.2), 6.92 (1H, dd, *J* = 8.8, 1.2), 7.13-7.12 (2H, m), 7.32-7.76 (3H, m),7.74 (1H, d, *J* = 8.5), 7.83 (1H, d, *J* = 4.4), 7.86 (1H, d, 4.7), 7.92 (1H, S); ^{13}C NMR (100 MHz, $CDCl_3$, 291 K) δ 106.3, 109.3, 110.8, 115.2, 115.5, 117.6, 124.0, 124.1, 124.7, 127.5, 128.4, 129.4, 130.4, 131.2, 131.4, 133.2,

134.9, 152.6, 153.4, 154.9; ESI-MS m/z: $[M]^{+1}$: 302.1 (molecular weight: 302.09 g/mol); FTIR 3389, 3049, 1650, 1611, 1564, 1480, 1340, 1238, 1198, 852, 774 cm^{-1}.

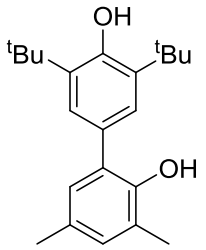

3,5-di-*tert*-butyl-3',5'-di-methyl-(1,1'-biphenyl)-4,2'-diol (1cd)[16] was obtained by column chromatography on silica gel using ethyl acetate-hexanes : light brown semi solid; up to 9% isolated column purified yield; ^{1}H NMR (400 MHz, $CDCl_3$, 291 K) δ 1.47 (18H, s), 2.28 (3H, s), 2.29 (3H, s), 5.22 (1H, broad, -OH), 5.31 (1H, broad, -OH), 6.87 (1H, s), 6.93 (1H, s), 7.22 (2H, s); ^{13}C NMR (100 MHz, $CDCl_3$, 291 K) δ 16.1, 20.4, 30.4, 34.5, 124.1, 125.7, 128.1, 128.2, 128.3, 129.0, 130.6, 136.9, 149.5, 153.6; ESI-MS m/z: $[M]^{+1}$: 326.1 (molecular weight: 326.18 g/mol); FTIR (cm^{-1}) 3393, 2947, 1479, 1430, 1338, 1196, 875, 767, 539 cm^{-1}.

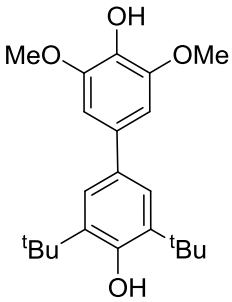

3,5-di-*tert*-butyl-3',5'-di-methoxy-(1,1'-biphenyl)-4,4'-diol (1ce)[42] was obtained by column chromatography on silica gel using ethyl acetate-hexanes : Yellow solid. Melting point 199-200°C; up to 72% isolated column purified yield; ^{1}H NMR (400 MHz, $CDCl_3$, 291 K) δ 1.39 (18H, s), 3.97 (6H, s), 7.00 (2H, s), 7.63 (2H, s); ^{13}C NMR (100 MHz, $CDCl_3$, 291 K) δ 29.3, 29.6, 29.7, 36.0, 55.8, 104.1, 125.6, 135.0, 150.0, 153.3; ESI-MS m/z: $[M-1]^{+1}$: 357.1 (molecular weight: 358.21 g/mol); FTIR 3510, 3016, 2947, 1605, 1504, 1442, 1342, 1295, 1211, 1080, 833, 702 cm^{-1} .

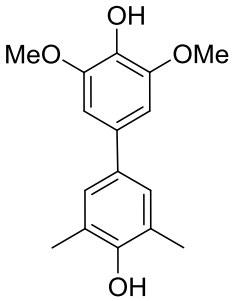

3,5-di-methoxy-3',5'-di-methyl-(1,1'-biphenyl)-4,4'-diol (1eh) was obtained by column chromatography on silica gel using ethyl acetate-hexanes : brown semi solid; up to 16% isolated column purified yield; ^{1}H NMR (400 MHz, $CDCl_3$, 291 K) δ 2.32 (6H, s), 3.95(6H, s), 4.68(1H, broad, -OH), 5.14(1H, broad, -OH), 6.75 (2H, s), 7.22 (2H, s); ^{13}C NMR (100 MHz, $CDCl_3$, 291 K) δ 16.1, 56.6 103.8, 124.1, 127.5, 133.0, 133.8, 133.9, 147.0, 151.6; ESI-MS m/z: $[M]^{+1}$: 274.7 (molecular weight: 274.12 g/mol); FTIR 3414, 2998, 1601, 1520, 1320, 1260, 880, 830 cm^{-1}.

3,5-di-*tert*-butyl-3',5'-di-methyl-[1,1'-biphenyl]-4,4'-diol (1ch)[13,42] was obtained as yellow semi solid, on analyzing with ESI-MS $[M+1]^{+1}$ m/z: 327.6 (molecular weight : 326.48 g/mol) was observed. Apart from that ESI-MS m/z: $[M-1]^{+1}$: 324.0 (molecular weight : 324.46 g/mol) was also observed may be due to its' Quinone form 2ch (3,5-di-*tert*-butyl-3',5'-di-methyl-[1,1'-bi(cyclohexylidene)]-2,2',5,5'-tetraene-4,4'-dione.

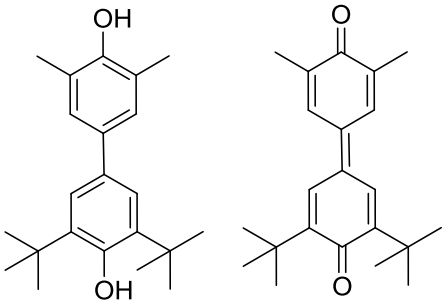

1ch 2ch

3.6 Spectral Data

3.6.1 FT-NMR (^{1}H and ^{13}C) spectral data

Figure F3.6.1 FT-NMR (^{1}H and ^{13}C) spectra of 1ac

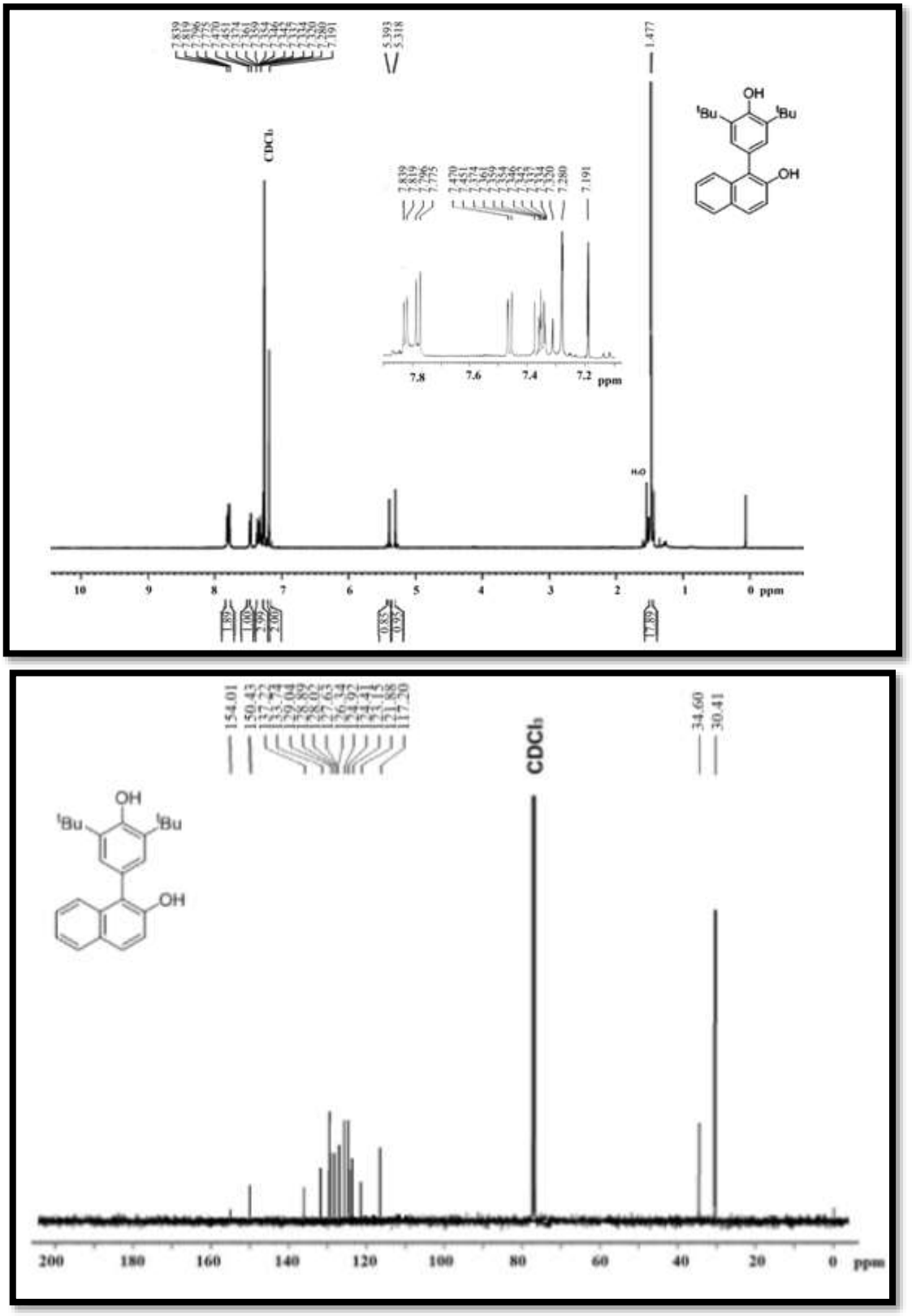

Figure F3.6.2 FT-NMR (^{1}H and ^{13}C) spectra of 1ae

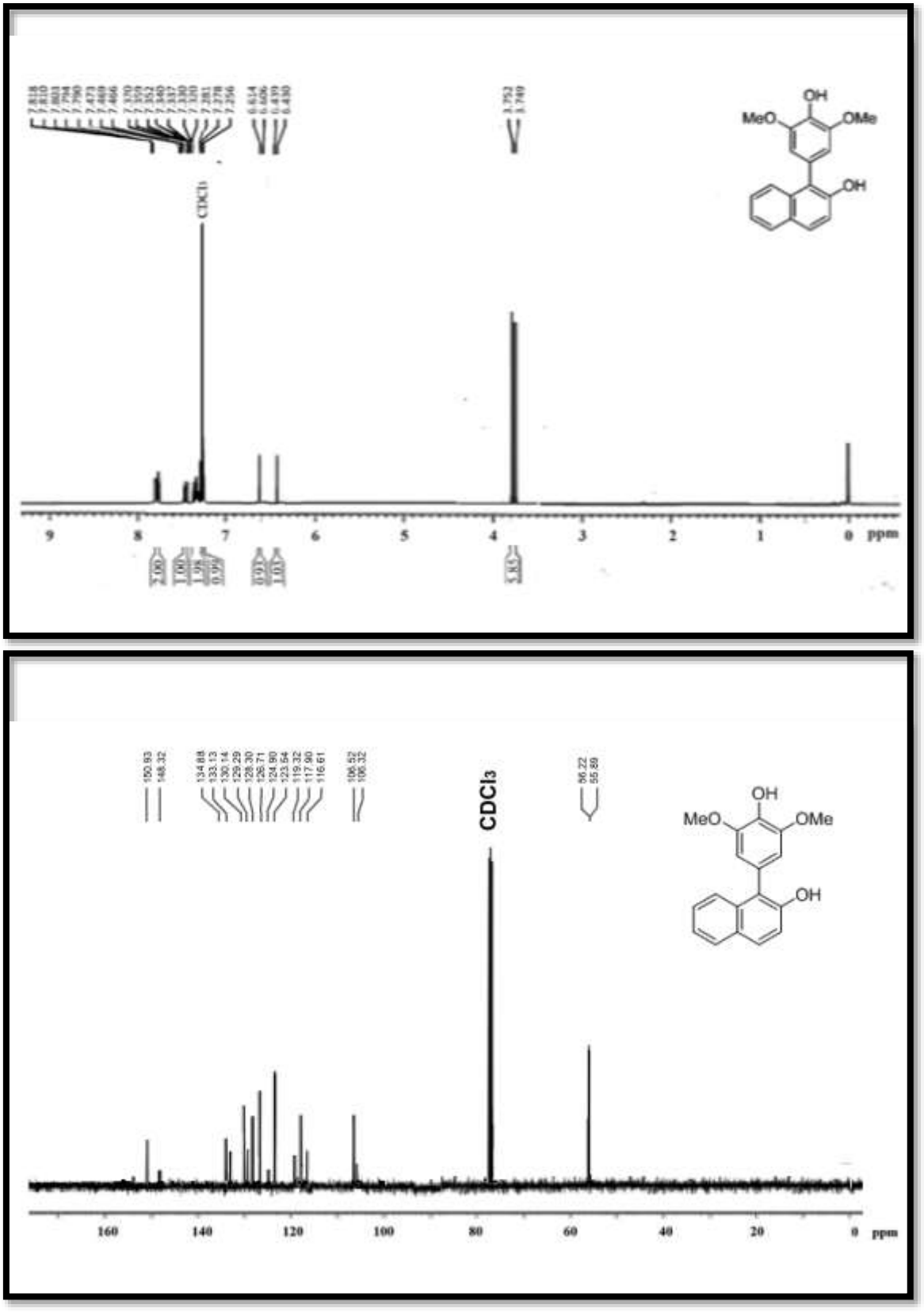

Figure F3.6.3 FT-NMR (^{1}H and ^{13}C) spectra of 1ag

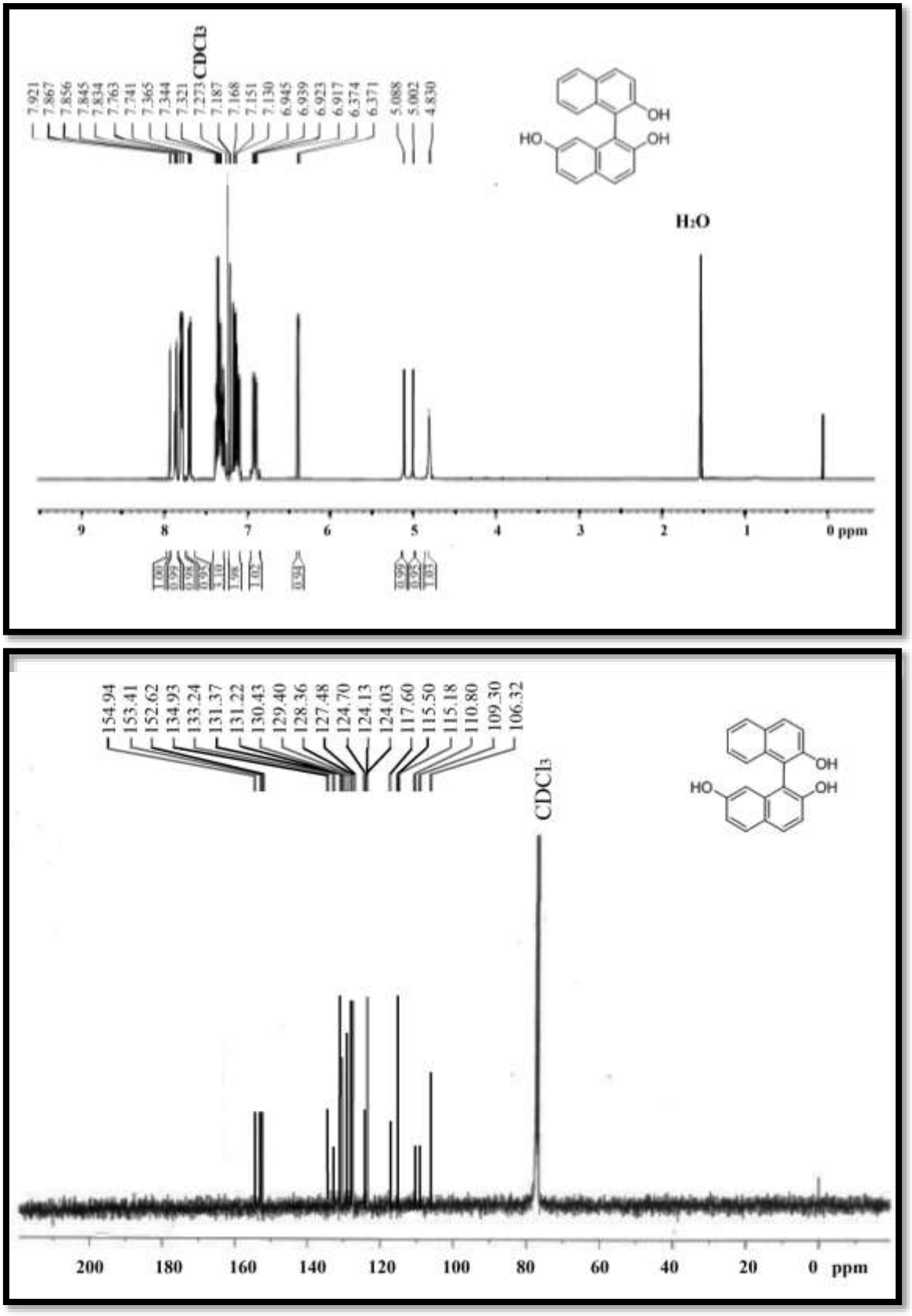

Figure F3.6.4 FT-NMR (^{1}H and ^{13}C) spectra of 1cd

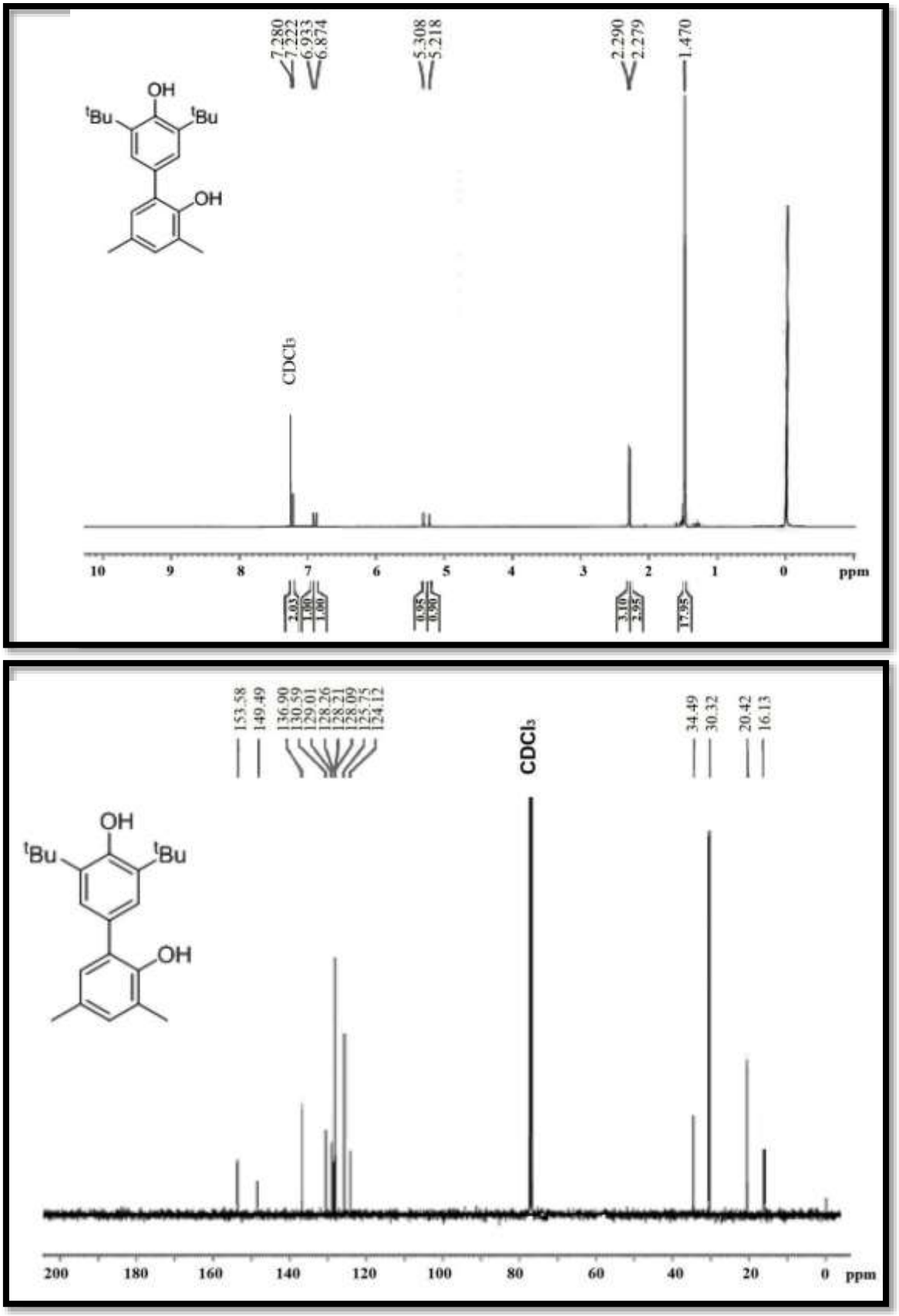

Figure F3.6.5 FT-NMR (^{1}H and ^{13}C) spectra of 1ce

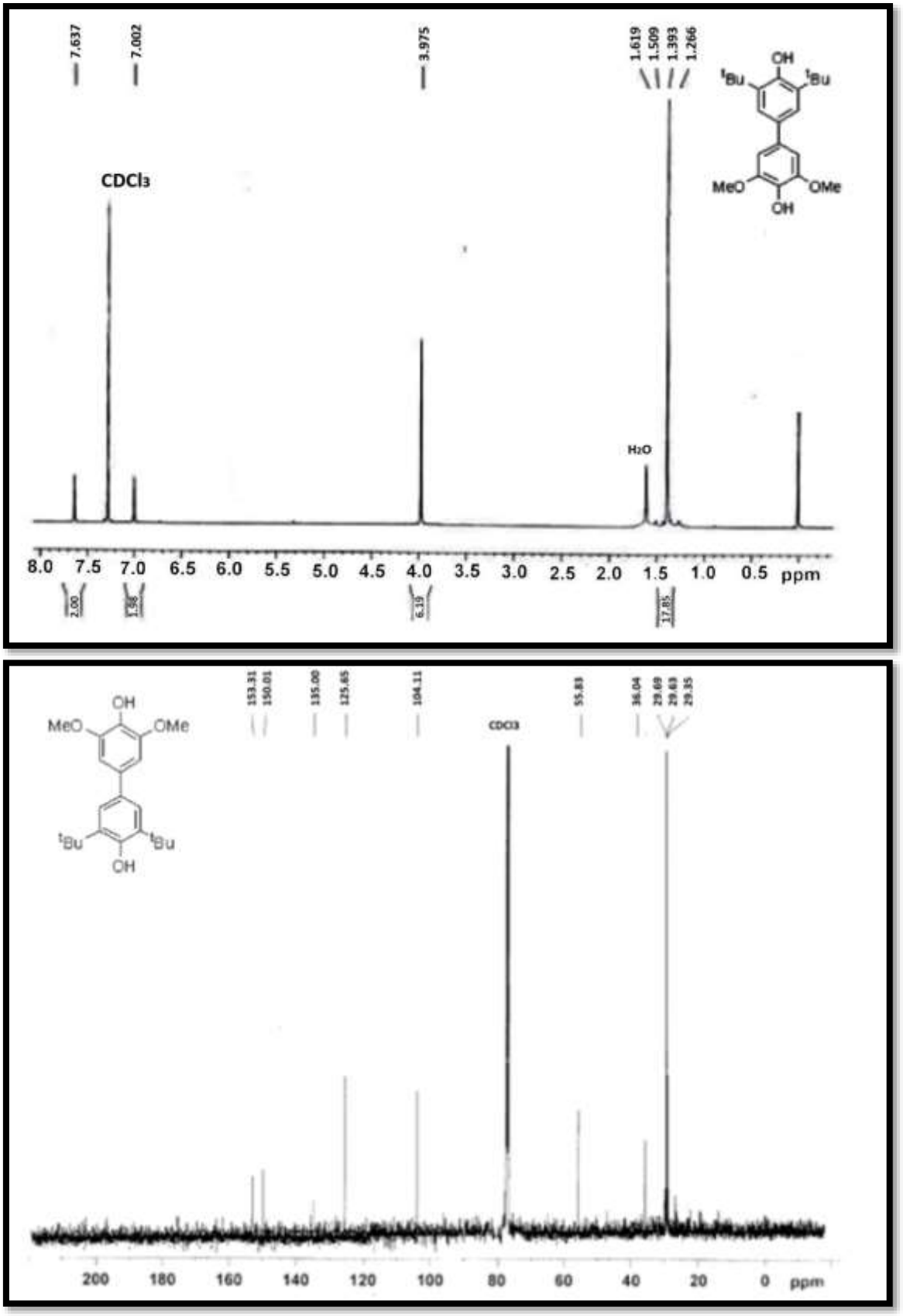

Figure F3.6.6 FT-NMR (^{1}H and ^{13}C) spectra of 1eh

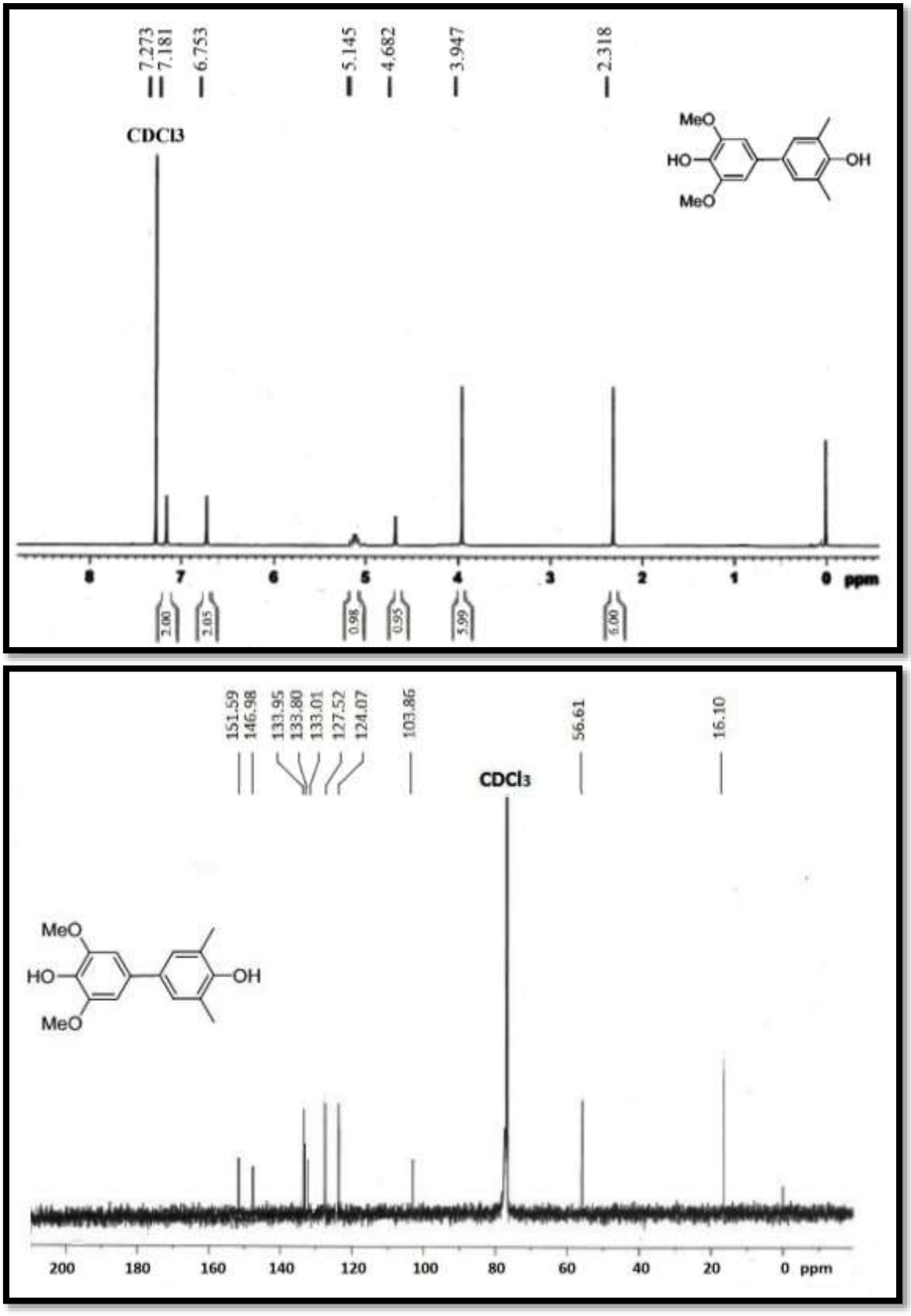

3.6.2 Mass spectrometry data

Figure F3.6.7 ESI-MS spectra of 1ac

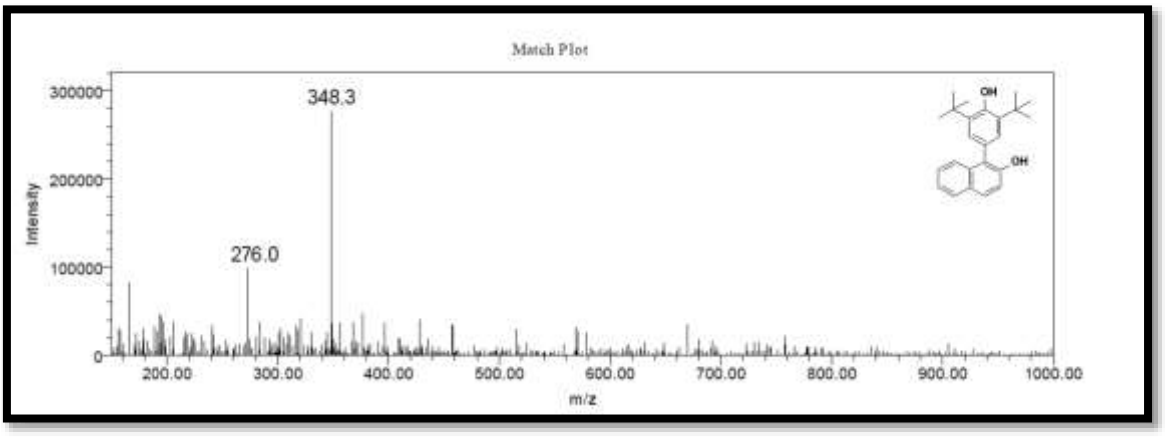

Figure F3.6.8 ESI-MS spectra of 1ae

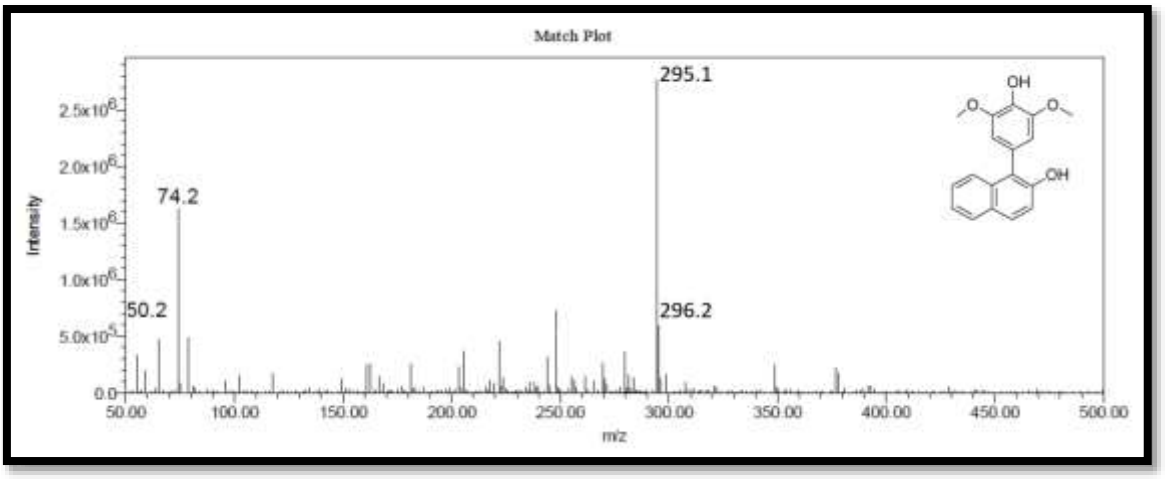

Figure F3.6.9 ESI-MS spectra of 1ag

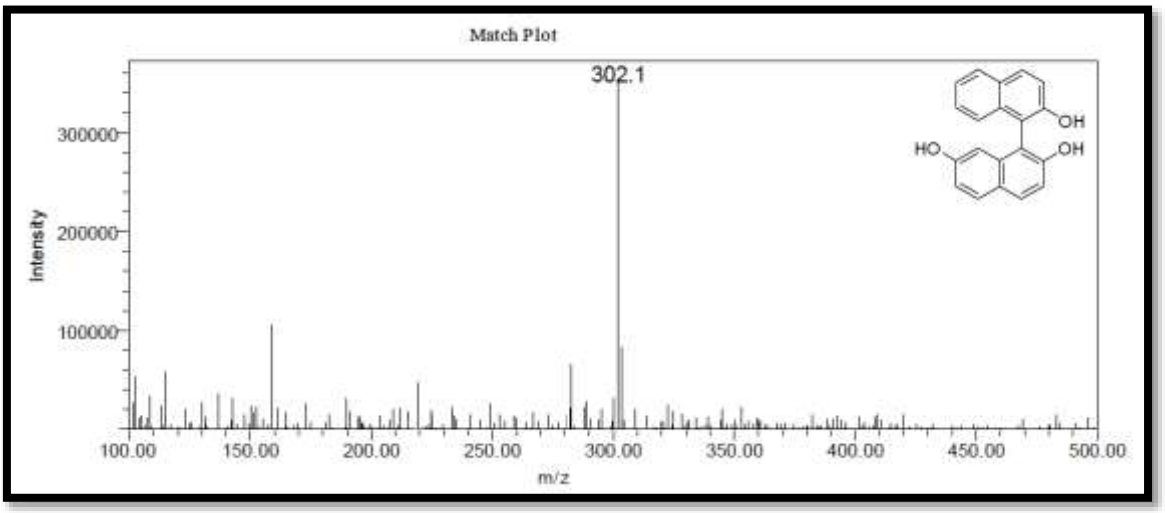

Figure F3.6.10 ESI-MS spectra of 1cd

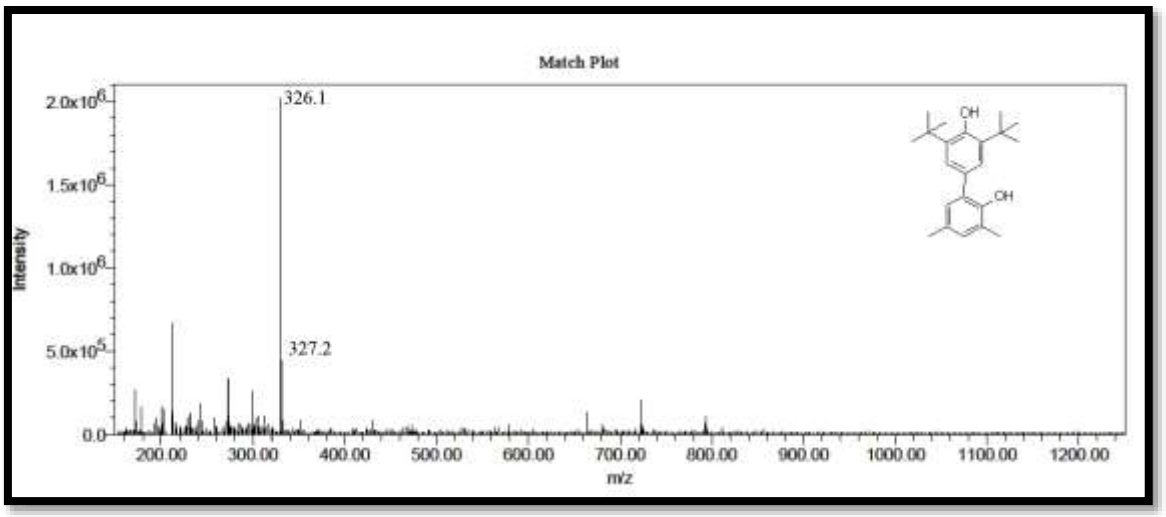

Figure F3.6.11 ESI-MS spectra of 1ce

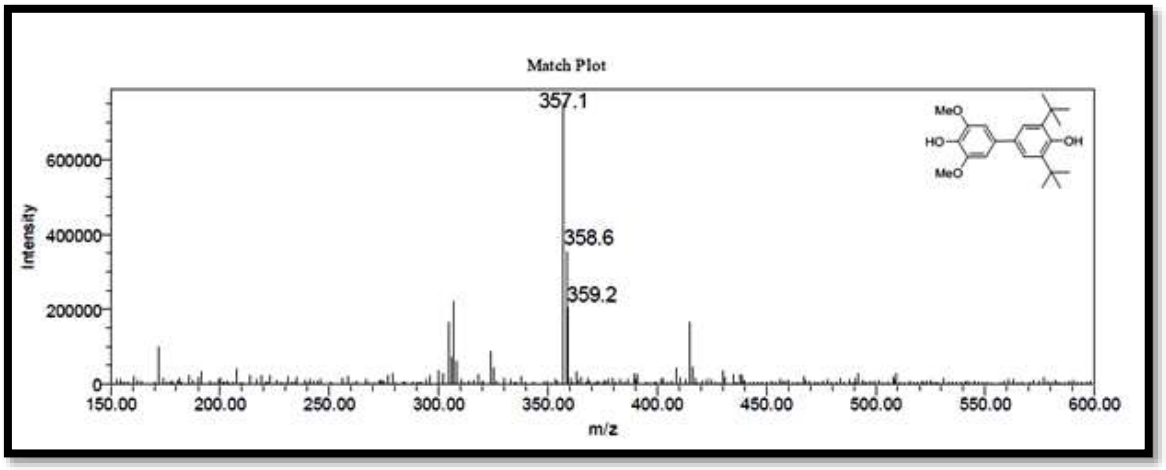

Figure F3.6.12 ESI-MS spectra of 1eh

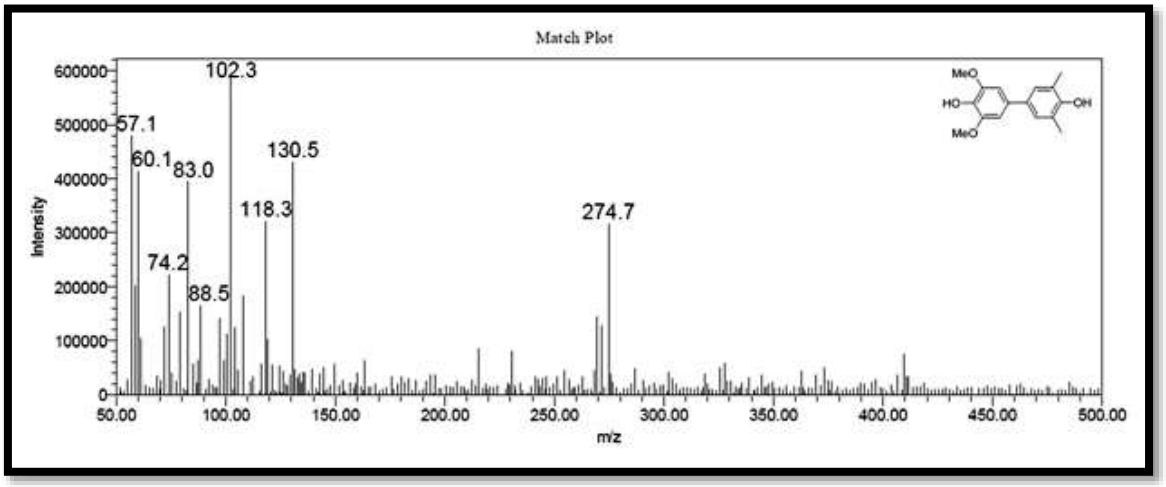

Figure F3.6.13 ESI-MS spectra of 1cd and 2cd

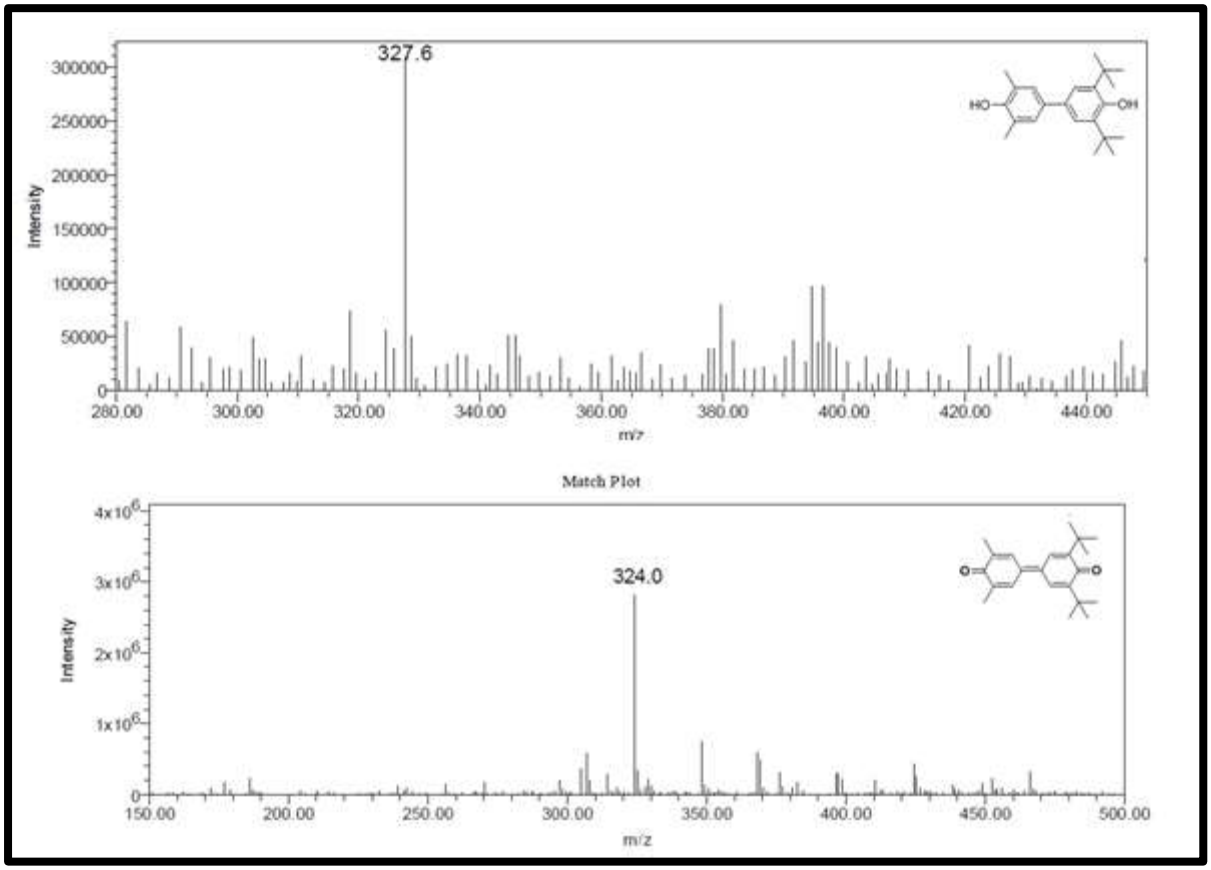

3.6.3 FT-IR spectral data

Figure F3.6.14 FT-IR spectra of 1ac

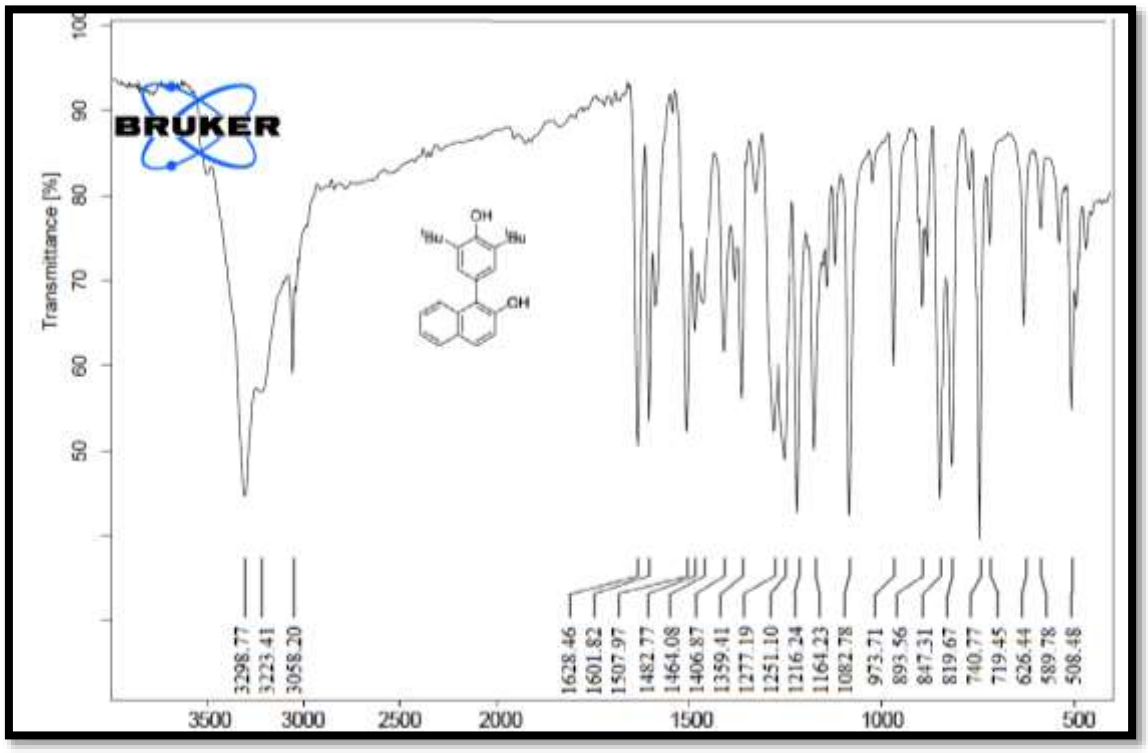

Figure F3.6.15 FT-IR spectra of 1ae

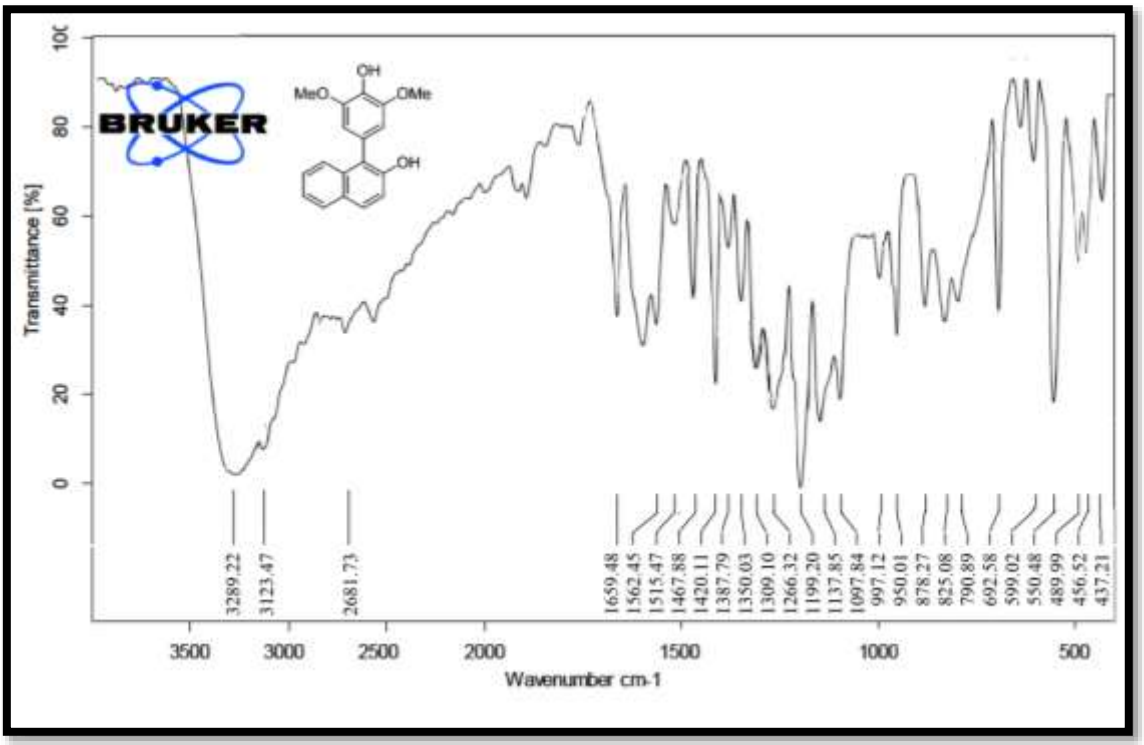

Figure F3.6.16 FT-IR spectra of 1ag

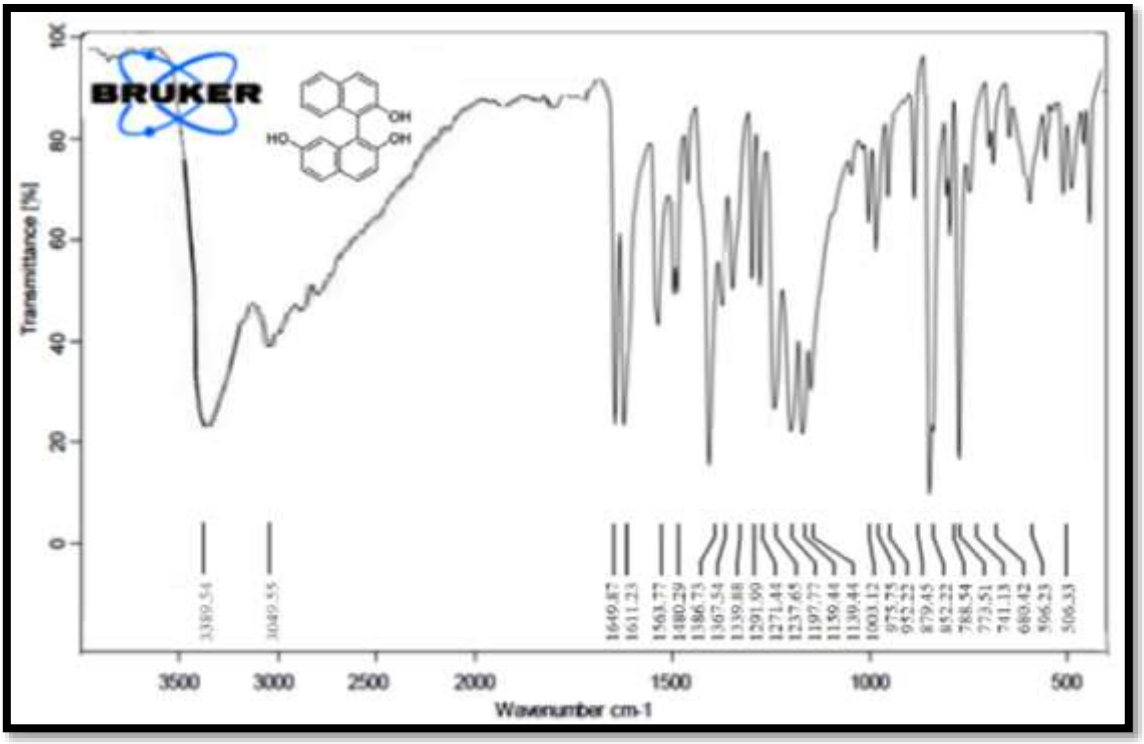

Figure F3.6.17 FT-IR spectra of 1cd

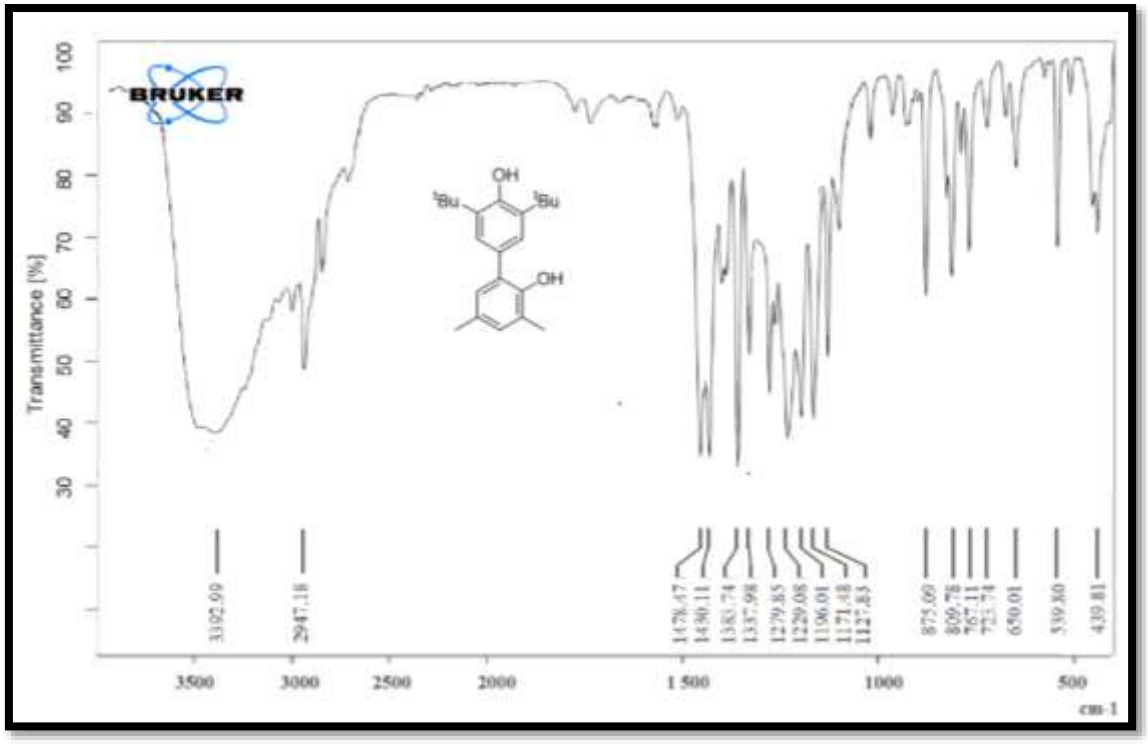

Figure F3.6.18 FT-IR spectra of 1ce

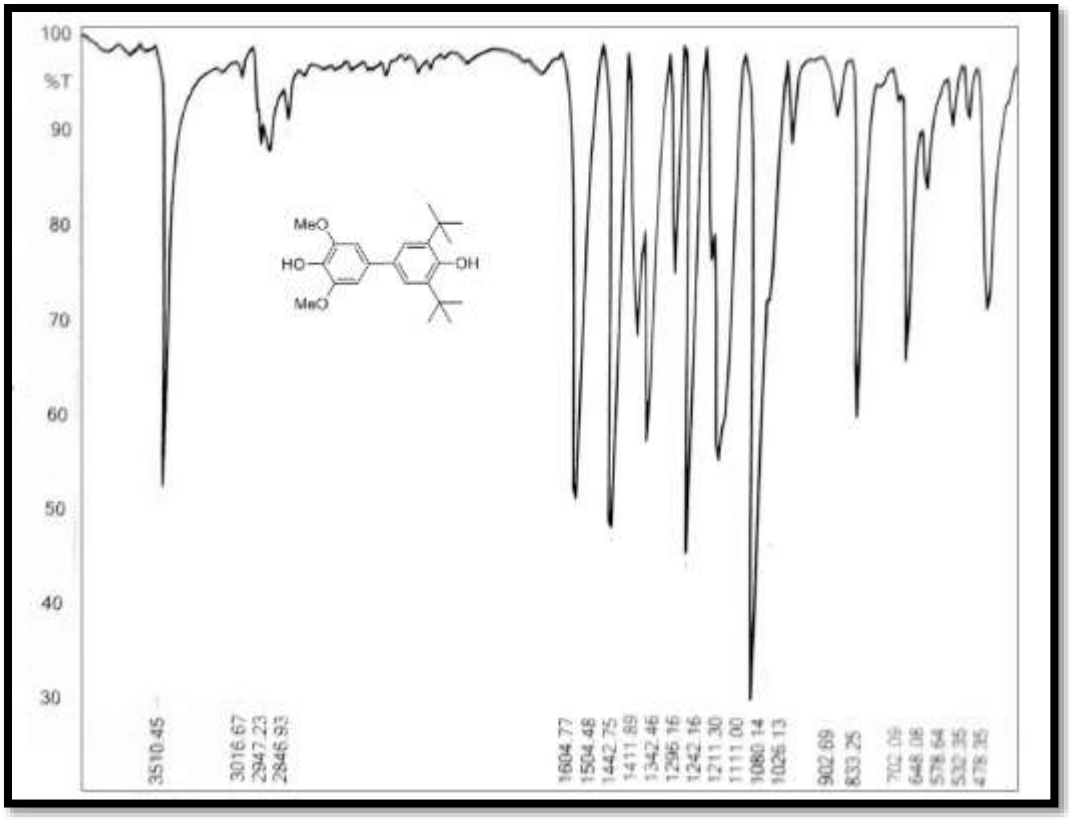

Figure F3.6.19 FT-IR spectra of 1eh

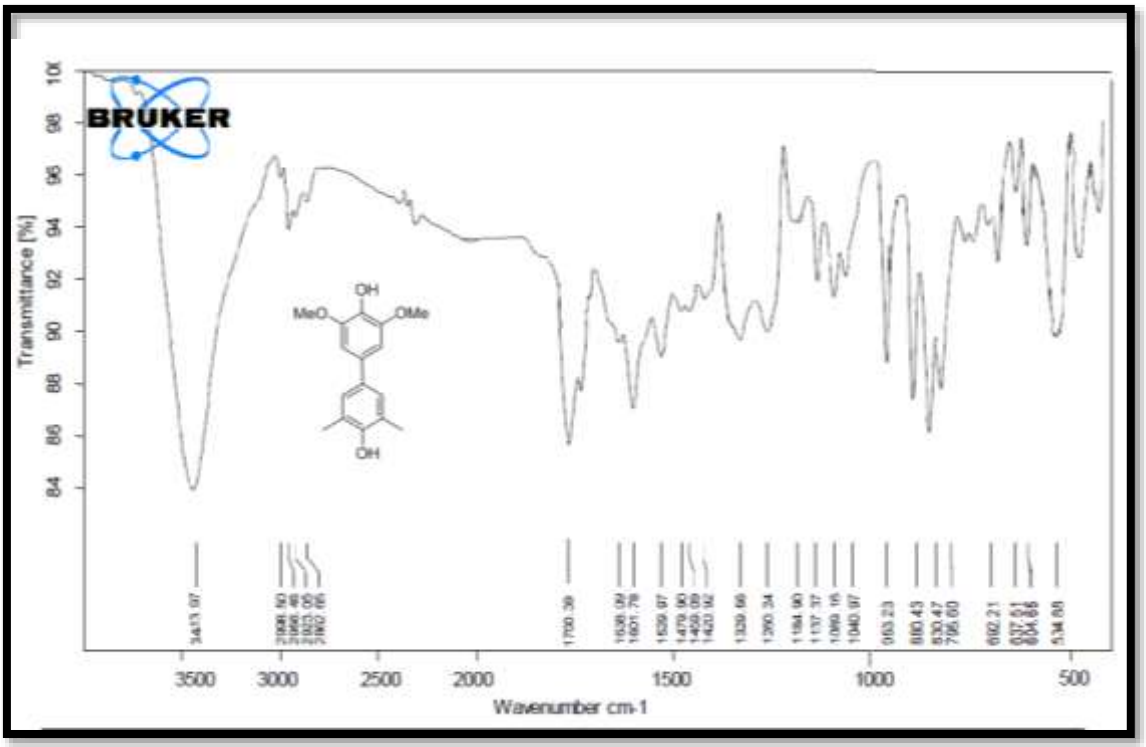

References

(1) Johansson Seechurn, C. C.; Kitching, M. O.; Colacot, T. J.; Snieckus, V. Palladium-Catalyzed Cross-Coupling: A Historical Contextual Perspective to the 2010 Nobel Prize. *Angew. Chemie - Int. Ed.* **2012**, *51* (21), 5062–5085.

(2) Kanwal, I.; Mujahid, A.; Rasool, N.; Rizwan, K.; Malik, A.; Ahmad, G.; Shah, S. A. A.; Rashid, U.; Nasir, N. M. Palladium and Copper Catalyzed Sonogashira Cross Coupling an Excellent Methodology for C-C Bond Formation over 17 Years: A Review. *Catalysts* **2020**, *10* (4), 443.

(3) Kočovský, P.; Vyskočil, Š.; Smrcina, M. Non-Symmetrically Substituted 1, 1 '-Binaphthyls in Enantioselective Catalysis. *Chem. Rev.* **2003**, *103* (8), 3213–3246.

(4) Lee, Y. E.; Cao, T.; Torruellas, C.; Kozlowski, M. C. Selective Oxidative Homo-and Cross-Coupling of Phenols with Aerobic Catalysts. *J. Am. Chem. Soc.* **2014**, *136* (19), 6782–6785.

(5) Hovorka, M.; Ščigel, R.; Gunterová, J.; Tichý, M.; Závada, J. The Oxidative Cross-Coupling of Substituted 2-Naphthols, Part I: The Scope and Limitations. *Tetrahedron* **1992**, *48* (43), 9503–9516.

(6) Libman, A.; Shalit, H.; Vainer, Y.; Narute, S.; Kozuch, S.; Pappo, D. Synthetic and Predictive Approach to Unsymmetrical Biphenols by Iron-Catalyzed Chelated Radical-Anion Oxidative Coupling. *J. Am. Chem. Soc.* **2015**, *137* (35), 11453–11460.

(7) Niederer, K.; Gilmartin, P. H.; Kozlowski, M. Oxidative Photocatalytic Homo-and Cross-Coupling of Phenols: Non-Enzymatic, Catalytic Method for Coupling Tyrosine. *ACS Catal.* **2020**, *10* (24), 14615–14623.

(8) Vareka, M.; Dahms, B.; Lang, M.; Hoang, M. H.; Trobe, M.; Weber, H.; Hielscher, M. M.; Waldvogel, S. R.; Breinbauer, R. Synthesis of a Bcl9 Alpha-Helix Mimetic for Inhibition of Ppis by a Combination of Electrooxidative Phenol Coupling and Pd-Catalyzed Cross Coupling. *Catalysts* **2020**, *10* (3), 340.

(9) Röckl, J. L.; Pollok, D.; Franke, R.; Waldvogel, S. R. A Decade of Electrochemical Dehydrogenative C,C-Coupling of Aryls. *Acc. Chem. Res.* **2020**, *53* (1), 45–61.

(10) Morimoto, K.; Sakamoto, K.; Ohshika, T.; Dohi, T.; Kita, Y. Organo-Iodine(III)-Catalyzed Oxidative Phenol-Arene and Phenol-Phenol Cross-Coupling Reaction. *Angew. Chemie Int. Ed.* **2016**, *55* (11), 3652–3656.

(11) He, Z.; Perry, G. J. P.; Procter, D. J. Sulfoxide-Mediated Oxidative Cross-Coupling of Phenols. *Chem. Sci.* **2020**, *11* (7), 2001–2005.

(12) Schulz, L.; Waldvogel, S. R. Solvent Control in Electro-Organic Synthesis. *Synlett* **2019**, *30* (3), 275–285.

(13) Schön, F.; Kaifer, E.; Himmel, H. J. Catalytic Aerobic Phenol Homo- and Cross-Coupling Reactions with Copper Complexes Bearing Redox-Active Guanidine Ligands. *Chem. - A Eur. J.* **2019**, *25* (35), 8279–8288.

(14) Shalit, H.; Libman, A.; Pappo, D. Meso-Tetraphenylporphyrin Iron Chloride Catalyzed Selective Oxidative Cross-Coupling of Phenols. *J. Am. Chem. Soc.* **2017**, *139* (38), 13404–13413.

(15) Reiss, H.; Shalit, H.; Vershinin, V.; More, N. Y.; Forckosh, H.; Pappo, D. Cobalt(II)[Salen]-Catalyzed Selective Aerobic Oxidative Cross-Coupling between Electron-Rich Phenols and 2-Naphthols. *J. Org. Chem.* **2019**, *84* (12), 7950–7960.

(16) Shalit, H.; Dyadyuk, A.; Pappo, D. Selective Oxidative Phenol Coupling by Iron Catalysis. *J. Org. Chem.* **2019**, *84* (4), 1677–1686.

(17) Colomer, I.; Chamberlain, A. E. R.; Haughey, M. B.; Donohoe, T. J. Hexafluoroisopropanol as a Highly Versatile Solvent. *Nat. Rev. Chem.* **2017**, *1* (11), 1–12.

(18) More, N.; Jeganmohan, M. Solvent-Controlled Selective Synthesis of Biphenols and Quinones via Oxidative Coupling of Phenols. *Chem. Commun.* **2017**, *53* (69), 9616–9619.

(19) Grzybowski, M.; Sadowski, B.; Butenschön, H.; Gryko, D. T. Synthetic Applications of Oxidative Aromatic Coupling—From Biphenols to Nanographenes. *Angew. Chemie - Int. Ed.* **2020**, *59* (8), 2998–3027.

(20) Gleede, B.; Selt, M.; Gütz, C.; Stenglein, A.; Waldvogel, S. R. Large, Highly Modular Narrow-Gap Electrolytic Flow Cell and Application in Dehydrogenative Cross-Coupling of Phenols. *Org. Process Res. Dev.* **2019**, *24* (10), 1916–1926.

(21) Gilmartin, P. H.; Kozlowski, M. C. Vanadium-Catalyzed Oxidative Intramolecular Coupling of Tethered Phenols: Formation of Phenol-Dienone Products. *Org. Lett.* **2020**, *22* (8), 2914–2919.

(22) Zaier, M.; Vidal, L.; Hajja, S.; Balan, L. Generating Highly Reflective and Conductive Metal Layers through a Light-Assisted Synthesis and Assembling of Silver Nanoparticles in a Polymer Matrix. *Sci. Rep.* **2017**, *7* (1), 1–10.

(23) Chadha, R.; Maiti, N.; Kapoor, S. Catalytic Reactions on the Surface of Ag Nanoparticles: A Photochemical Effect and/or Molecule Property? *J. Phys. Chem. C*

2014, *118* (45), 26227–26235.

(24) Kong, H.; Yang, S.; Gao, H.; Timmer, A.; Hill, J. P.; Díaz Arado, O.; Mönig, H.; Huang, X.; Tang, Q.; Ji, Q.; et al. Substrate-Mediated C-C and C-H Coupling after Dehalogenation. *J. Am. Chem. Soc.* **2017**, *139* (10), 3669–3675.

(25) Bratlie, K. M.; Lee, H.; Komvopoulos, K.; Yang, P.; Somorjai, G. A. Platinum Nanoparticle Shape Effects on Benzene Hydrogenation Selectivity. *Nano Lett.* **2007**, *7* (10), 3097–3101.

(26) Huang, L.; Zhang, X.; Wang, Q.; Han, Y.; Fang, Y.; Dong, S. Shape-Control of Pt-Ru Nanocrystals: Tuning Surface Structure for Enhanced Electrocatalytic Methanol Oxidation. *J. Am. Chem. Soc.* **2018**, *140* (3), 1142–1147.

(27) Corma, A.; Concepción, P.; Boronat, M.; Sabater, M. J.; Navas, J.; Yacaman, M. J.; Larios, E.; Posadas, A.; López-Quintela, M. A.; Buceta, D.; et al. Exceptional Oxidation Activity with Size-Controlled Supported Gold Clusters of Low Atomicity. *Nat. Chem.* **2013**, *5* (9), 775–781.

(28) Liu, L.; Corma, A. Metal Catalysts for Heterogeneous Catalysis: From Single Atoms to Nanoclusters and Nanoparticles. *Chem. Rev.* **2018**, *118*, 4981–5079.

(29) Jiang, Q.; Li, J. C.; Chi, B. Q. Size-Dependent Cohesive Energy of Nanocrystals. *Chem. Phys. Lett.* **2002**, *366* (5–6), 551–554.

(30) Chow, T. S. Size-Dependent Adhesion of Nanoparticles on Rough Substrates. *J. Phys. Condens. Matter* **2003**, *15* (2), L-83-L–87.

(31) Xiong, R.; Luan, J.; Kang, S.; Ye, C.; Singamaneni, S.; Tsukruk, V. V. Biopolymeric Photonic Structures: Design, Fabrication, and Emerging Applications. *Chem. Soc. Rev.* **2020**, *49* (3), 983–1031.

(32) Gal, A.; Weiner, S.; Addadi, L. A Perspective on Underlying Crystal Growth Mechanisms in Biomineralization: Solution Mediated Growth versus Nanosphere Particle Accretion. *CrystEngComm* **2015**, *17* (13), 2606–2615.

(33) De Yoreo, J. J.; Gilbert, P. U. P. A.; Sommerdijk, N. A. J. M.; Penn, R. L.; Whitelam, S.; Joester, D.; Zhang, H.; Rimer, J. D.; Navrotsky, A.; Banfield, J. F.; et al. Crystallization by Particle Attachment in Synthetic, Biogenic, and Geologic Environments. *Science* **2015**, *349* (6247), aaa6760.

(34) Thanh, N. T. K.; Maclean, N.; Mahiddine, S. Mechanisms of Nucleation and Growth of Nanoparticles in Solution. *Chem. Rev.* **2014**, *114* (15), 7610–7630.

(35) Xia, Y.; Xia, X.; Peng, H. C. Shape-Controlled Synthesis of Colloidal Metal

Nanocrystals: Thermodynamic versus Kinetic Products. *J. Am. Chem. Soc.* **2015**, *137* (25), 7947–7966.

(36) Zeng, J.; Xia, X.; Rycenga, M.; Henneghan, P.; Li, Q.; Xia, Y. Successive Deposition of Silver on Silver Nanoplates: Lateral versus Vertical Growth. *Angew. Chemie - Int. Ed.* **2011**, *50* (1), 244–249.

(37) Hemmingson, S. L.; Campbell, C. T. Trends in Adhesion Energies of Metal Nanoparticles on Oxide Surfaces: Understanding Support Effects in Catalysis and Nanotechnology. *ACS Nano* **2017**, *11* (2), 1196–1203.

(38) Anderson, T. H.; Yu, J.; Estrada, A.; Hammer, M. U.; Waite, J. H.; Israelachvili, J. N. The Contribution of DOPA to Substrate-Peptide Adhesion and Internal Cohesion of Mussel-Inspired Synthetic Peptide Films. *Adv. Funct. Mater.* **2010**, *20* (23), 4196–4205.

(39) Bhanderi, K.; Ghalsasi, P. S.; Inoue, K. Nonconventional Driving Force for Selective Oxidative C–C Coupling Reaction Due to Concurrent and Curious Formation of Ag0. *Sci. Rep.* **2021**, *11* (1), 1–11.

(40) More, N. Y.; Jeganmohan, M. Oxidative Cross-Coupling of Two Different Phenols: An Efficient Route to Unsymmetrical Biphenols. *Org. Lett.* **2015**, *17* (12), 3042–3045.

(41) Narute, S.; Parnes, R.; Toste, F. D.; Pappo, D. Enantioselective Oxidative Homocoupling and Cross-Coupling of 2 - Naphthols Catalyzed by Chiral Iron Phosphate Complexes. *J. Am. Chem. Soc.* **2016**, *138* (50), 16553-16560.

(42) Nishino, H.; Itoh, N.; Nagashima, M.; Kurosawa, K. Choice of Manganese(Iii) Complexes for the Synthesis of 4,4′-Biphenyldiols and 4,4′-Diphenoquiones. *Bulletin of the Chemical Society of Japan*. 1992, pp 620–622.